



Molecular Crystals and Liquid Crystals

Publication details, including instructions for authors and subscription information:

<http://www.tandfonline.com/loi/gmcl16>

Temperature Dependence of Tilt, Pitch and Polarization in Ferroelectric Liquid crystals

Ph. Martinot-lagarde^a, R. Duke^a & G. Durand^a

^a Laboratoire de Physique de Solides, Université de Paris-Sud, 94105, Orsay, France

Version of record first published: 14 Oct 2011.

To cite this article: Ph. Martinot-lagarde, R. Duke & G. Durand (1981): Temperature Dependence of Tilt, Pitch and Polarization in Ferroelectric Liquid crystals, *Molecular Crystals and Liquid Crystals*, 75:1, 249-286

To link to this article: <http://dx.doi.org/10.1080/00268948108073619>

PLEASE SCROLL DOWN FOR ARTICLE

Full terms and conditions of use: <http://www.tandfonline.com/page/terms-and-conditions>

This article may be used for research, teaching, and private study purposes. Any substantial or systematic reproduction, redistribution, reselling, loan, sub-licensing, systematic supply, or distribution in any form to anyone is expressly forbidden.

The publisher does not give any warranty express or implied or make any representation that the contents will be complete or accurate or up to date. The accuracy of any instructions, formulae, and drug doses should be independently verified with primary sources. The publisher shall not be liable for any loss, actions, claims, proceedings, demand, or

costs or damages whatsoever or howsoever caused arising directly or indirectly in connection with or arising out of the use of this material.

Temperature Dependence of Tilt, Pitch and Polarization in Ferroelectric Liquid Crystals

PH. MARTINOT-LAGARDE, R. DUKE and G. DURAND

Laboratoire de Physique des Solides, Université de Paris-Sud, 91405 Orsay, France

(Received January 14, 1981)

We present temperature measurements of the important parameters defining the properties of the smectic C* phase in a series of schiff bases. The pitch of the helical texture is measured optically. The molecular tilt is deduced from optical observations and from X-ray measurements of the smectic layer thickness. The critical electric field for unwinding of the helical texture is measured in the homeotropic and planar geometries. With these data, the spontaneous polarization is estimated to be in the range of 10^{-3} Debye/molecule/radian, excepted for HOBACPC, a compound with a chlorine directly fixed on the asymmetric carbon, where it is one order of magnitude larger. Intramolecular rotations appear as an important factor to decrease the spontaneous polarization.

INTRODUCTION

The symmetry of most liquid crystal phases¹ prevents the appearance of ferroelectricity. R. Meyer *et al.*² have shown in 1975 that chiral compounds in the smectic C* phase can exhibit a spontaneous electric polarization, in the plane of the smectic layers. In the higher temperature smectic A phase of a chiral compound, where the molecules are normal to the smectic layers, there is a center of inversion and no ferroelectricity. The molecular tilt in the C* phase allows the appearance of the spontaneous polarization and is the important (order) parameter of the problem. Because of the molecular chirality, the C* phase presents an helical texture, with a pitch of the order of a few microns. By applying an electric field which couples to the spontaneous polarization, one can unwind the helix. This allows the measurement of the spontaneous polarization, if the helical pitch is known.

In this paper, we have measured these three important parameters: molecular tilt, pitch and unwinding critical field, in smectic C* compounds, versus the temperature. This allows us to estimate the spontaneous electric polarization

versus temperature. We have made these measurements on a series of 7 schiff base compounds,³ the DOBAMBC, PACMB, OOBAMBMC, OOBAMBCC, DOBAMBCC and HOBACPC (see Table I). All these compounds present a smectic A to smectic C* transition, which is continuous (second order) except for the PACMB which appears weakly first order.³ An important point is to make an eventual connection between the molecular structure of these compounds and the macroscopic properties of the ferroelectric phase. All these compounds are chiral because of the presence of one asymmetric carbon on the aliphatic end chain (two for the PACMB, one at each chain end). The molecules present large transverse dipoles ($\text{N}=\text{O}$ in PACMB, $\text{C}\equiv\text{N}$ in DOBAMBCC, TDOBAMBCC, the common $\text{C}=\text{O}$ group for the other compounds). In most cases, these dipoles are placed at random along the molecular chain. In one case, for HOBACPC, the transverse dipole is a chlorine directly fixed on the asymmetric carbon. An eventual comparison between the macroscopic polarization of these compounds will be useful to understand the role of these dipoles.

Our paper is organized in four sections. We first recall some symmetry properties of the C* phase. We present the tilt angle from optical measurements and from X-ray determinations of smectic layer thickness. We give next our data concerning the pitch. The last section is devoted to the measurement of the critical field to unwind the helix, from which we deduce the spontaneous polarization. A few of these data have already been presented in a review paper.⁴

I SYMMETRY AND PROPERTIES OF THE CHIRAL C* PHASE

X-ray studies⁵ have shown that in the smectic C phase the molecules are arranged in layers, with their center of mass, randomly distributed in every layer. Their long axis are, on the average, parallel compared to each others and tilted compared to the layer normal. The plane containing the normal to the smectic layers and the long axis of the molecules is a mirror plane (Figure 1). All observations suggest that the normal to the mirror plane is a twofold axis with a randomly head to tail molecular distribution. EPR and NMR experiments have shown that the molecules can rotate around their long axis almost as rapidly as in the nematic phase. This rotation is hindered, and the smectic C is optically biaxial. The existence of a center of inversion prevents any spontaneous polarization to exist.

In a smectic C* phase, made with chiral molecules, optical observation² show that the smectic layers pile up on each other while twisting along the layer normal. This results in an helicoidal texture. That texture possesses no mirror plane anymore. The twofold axis is the only remaining symmetry element. If the individual molecules possess a permanent dipolar moment perpendicular to their long axis, then a macroscopic spontaneous electric polarization can exist along the twofold axis.

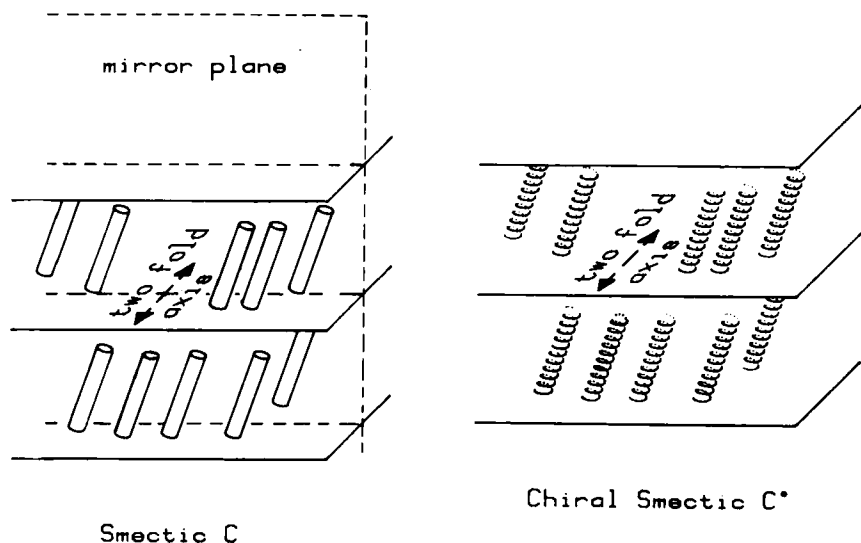


FIGURE 1 Symmetry of the chiral and non-chiral C phases.

Angular parameters symmetry

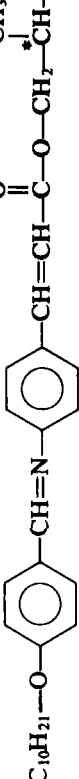
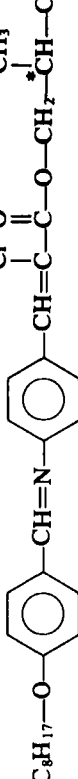
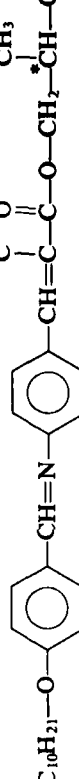
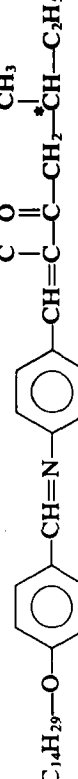
Let us define (Figure 2) an orthonormal reference frame (x, y, z) for the smectic layer and another one (ξ, η, ζ) related to the averaged molecules. Oz is chosen arbitrary normal to the smectic layers, Ox (and Oy) is arbitrary. $O\zeta$ is also arbitrary chosen along the long axis of the molecule. $O\xi$ arbitrary, aligned along the twofold symmetry axis, is perpendicular to Oz and $O\zeta$. As usual, one goes from the frame (x, y, z) to (ξ, η, ζ) by the rotation $\phi = (Ox, O\xi)$ along Oz , and the tilt $\theta = (Oz, O\zeta)$ measured along $O\xi$. The symmetry implies that:

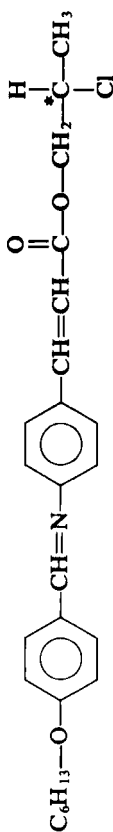
- 1) (ϕ, θ) and $(-\phi, \theta + \pi)$ are equivalent because of the arbitrary orientation of z .
- 2) (ϕ, θ) and $(\phi, \theta + \pi)$ are equivalent, because of the arbitrary orientation of ζ .
- 3) The origin of ϕ is arbitrary, because of the arbitrary choice of Ox .
- 4) Two couples of coordinate (ϕ, θ) and $(\phi + \pi, -\theta)$ are equivalent because of the arbitrary choice of $O\xi$.

The properties (1) and (2) are equivalent because of the twofold axis $O\xi$. Let us call P the unique ξ component of the local spontaneous polarization (per unit volume). (3) and (4) imply that P does not depend on ϕ and is an odd function of θ . We write $P = P_0\theta$ for small values of the tilt, as in Ref. 2.

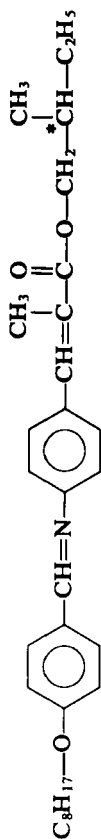
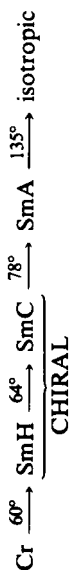
In a texture with homogeneous layers, z is the only variable. Because of (3) only the derivatives of ϕ compared to z have a physical meaning. The property (1) allows a nonzero value of the twist $\partial\phi/\partial z$, because ϕ changes its sign when z is reverted. At equilibrium, the texture is defined by an uniform twist

TABLE I

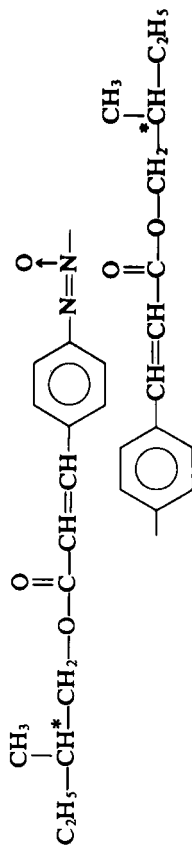
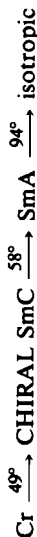
Compound and name	Thermal	Phase	Diagram
$C_{10}H_{21}-O-$  P-decyloxybenzylidene P'-amino 2 methyl butyl cinnamate (DOBAMBC)	$Cr \xrightarrow{76^\circ} CHIRAL\ SmC \xrightarrow{95^\circ} SmA \longrightarrow isotropic$ <div style="margin-left: 100px;"> $\swarrow 63^\circ$ SmH </div>		
$C_8H_{17}-O-$  P-octyloxybenzylidene P'-amino 2 methyl butyl α chloro cinnamate (OOBAMBCC)	$Cr \xrightarrow{27^\circ} CHIRAL\ SmC \xrightarrow{41^\circ} SmA \xrightarrow{66^\circ} isotropic$ <div style="margin-left: 100px;"> $\swarrow 38^\circ$ </div>		
$C_{10}H_{21}-O-$  P-decyloxybenzylidene P'-amino 2 methyl butyl α cyano cinnamate (DOBAMBCC)	$Cr \xrightarrow{70^\circ} CHIRAL\ SmC \xrightarrow{92^\circ} SmA \xrightarrow{104^\circ} isotropic$ <div style="margin-left: 100px;"> $\swarrow 75^\circ$ </div>		
$C_{14}H_{29}-O-$  P-tetradecyloxybenzylidene P'-amino 2 methyl butyl α cyano cinnamate (TDOBAMBCC)	$Cr \xrightarrow{47^\circ} CHIRAL\ SmC \xrightarrow{78^\circ} SmA \xrightarrow{105^\circ} isotropic$ <div style="margin-left: 100px;"> $\swarrow 70^\circ$ </div>		



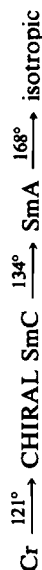
P-hexyloxybenzylidene P'-amino 2 chloro α propyle cinnamate
(HOBACPC)



P-octyloxybenzylidene P'-amino 2 methyl butyl α methyl cinnamate
(OOBAMBMC)



P-azoxy cinnamate methyl 2 butanol
(PACMB)



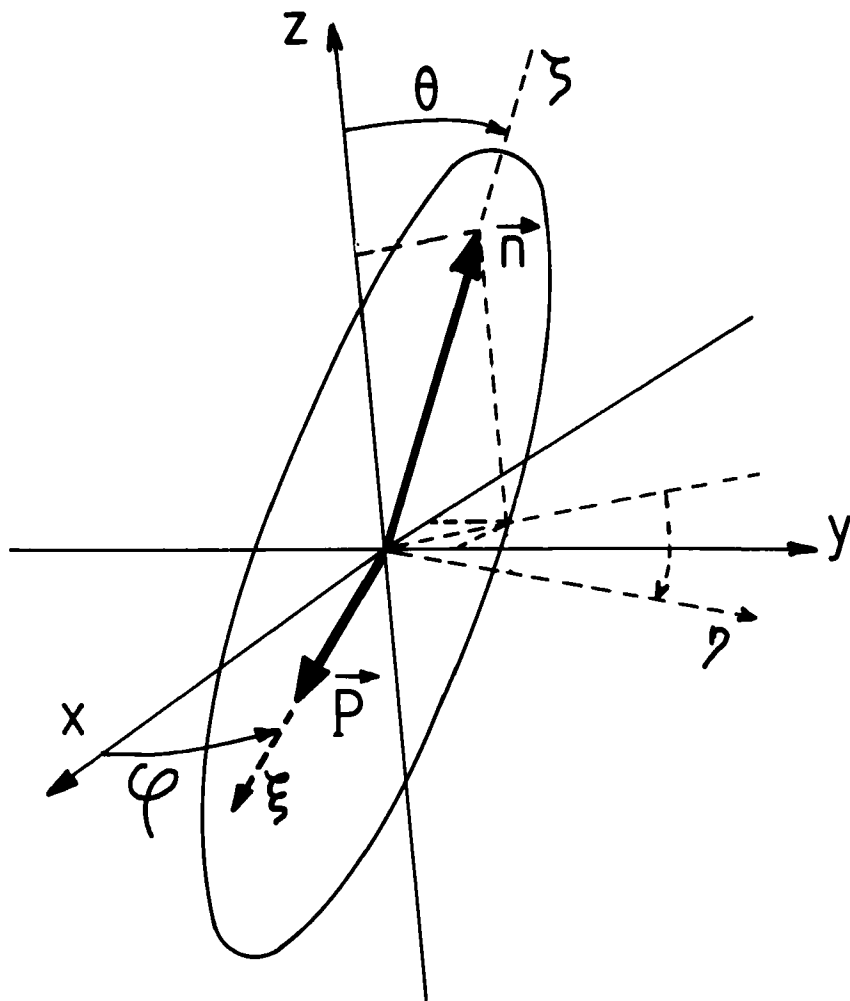


FIGURE 2 Geometry of reference frames.

$\partial\phi/\partial z = q_0$ resulting in an helicoidal conical texture. The corresponding pitch is $Z = 2\pi/q_0$. q_0 is an even function of θ , because of (4).

If the local twist of layers is not exactly equal to q_0 , it appears a free energy density:

$$F = \frac{1}{2} K \left(\frac{\partial\phi}{\partial z} - q_0 \right)^2$$

where K is some curvature elastic constant. The property (4) implies that K is also an even function of θ . In the limit of small θ , in the smectic A phase, there

cannot be any twist energy; as the twist $\partial\phi/\partial z$ can be arbitrary, K must vanish. We can write $K = K_0\theta^2$ for small tilt values. These expressions for P and K will be useful in next sections.

II MOLECULAR TILT MEASUREMENT

The tilt angle θ of molecules inside the smectic layers is the order parameter of the smectic C phase. It is also the order parameter of the C* phase, since in the chiral smectic C*, the permanent polarization P is itself proportional to θ . The point is that θ is not uniquely defined. θ represents the tilt of the long axis of any second rank tensor associated with the molecules, for instance the diamagnetic susceptibility or the dielectric or optical indices tensor.⁵ It is also possible to measure the tilt of the long axis of the mean inertial tensor of the electrons on one molecule, which can be obtained by X-rays. For rigid molecules, all these definitions are equivalent for small θ , within a factor of proportionality. For nonrigid molecules, we know⁶ that long flexible end chain can result in different apparent optical and X-ray tilts. In this work, we have measured the tilt angle for a series of homologues chiral C* compounds, using the two different techniques: the optical one, and the one derived from the X-ray layer thickness measurement with the rigid rod assumption.

X-ray measurements

The method we use is based, in absence of more information, on the rigid rod model to describe the molecules inside the layers. Calling d_0 the length of these rods, of negligible thickness, we can write obviously the real thickness in the C phase as $d = d_0 \cos \theta$. d can be obtained by making an X-ray powder diagram on an unoriented sample. d_0 is derived from the layer periodicity in the smectic A phase close to the transition temperature T_{CA} . Our experimental setup is conventional.⁵ The liquid crystal is placed on a platinum grid and supported by an aluminum foil backing. The sample is placed in a brass sample holder, mounted in the X-ray spectrometer. During exposure to a Cu K α X radiation, the entire sample assembly is tilted through a known angle. Sample temperature is maintained constant within $\pm 0.2^\circ\text{C}$ by circulating oil from a thermostated bath sample. The temperature is measured by a thermocouple mounted in the sample holder. A photographic exposure of one hour at 40 kV and 20 mA was found to be sufficient for measurement. The periodicity of the smectic layers is obtained from the X-ray photographs by measuring the separation between the lines formed by the beams scattered and non-scattered by the smectic layers, through the Bragg relation $\lambda = 2d \sin(\alpha/2)$ where λ is the wavelength of the Cu K α radiation (1.54 Å) and α the Bragg reflection angle. The variation of d is small close to the transition. It is then very difficult to

observe a possible discontinuity of θ close to T_c , i.e. to check by this method the order of the $A \rightarrow C^*$ transition for weakly first order compounds.

The tilt angle measurements have been made for four compounds, the DOBAMBC, OOBAMBMC, OOBAMBCC, TDOBAMBCC. The $S_A \rightarrow S_C$ transition temperatures T_c are in the range $38^\circ \rightarrow 95^\circ$. To take care of this variation, we have plotted the tilt angle versus ΔT , the departure from the transition temperature ($\Delta T = T - T_c$). Our results are shown on Figure 3. We note the large error bars close to T_c . The interesting result is that for these four compounds, θ presents the same temperature dependence, with about the same absolute values. This is not too surprising since the four compounds are chemically similar. The larger tilt is $\theta \sim 20^\circ$, for $T - T_c \sim -15^\circ$; at lower temperature, these compounds crystallize, except for the DOBAMBC which goes into a H phase. In a mean field model,¹ one expects the order parameter θ to vary in temperature according to the law $\theta = \theta_0(T_c - T)^\beta$ with $\beta = 0.5$. A non classical behavior⁷ would lead to $\beta = 0.35$. We have tried a power law fit to estimate the critical exponent β from our data. The problem of this fit is the one of the T_c determination, because T_c is not measured directly by the X-rays experiment. For each compound, we have made a least square adjustment of our data on a law of the form: $\theta = \theta_0(T_c - T)^\beta$, with θ_0 , T_c and β as adjustable parameters. The best values for θ_0 and β are shown on Table II. r^2 is the usual determination coefficient.⁸

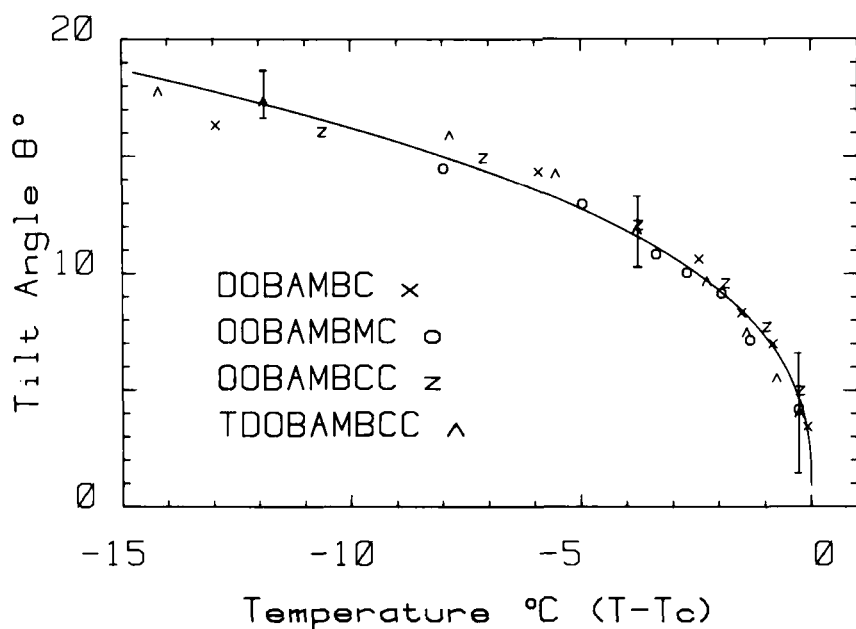


FIGURE 3 Tilt angle versus reduced temperature, from X-ray data.

TABLE II

Tilt angle (in degree) versus temperature (in degree C)

$$\theta = \theta_o(T_c - T)^\beta$$

Compound	Method	θ_o	β	r^2
DOBAMBC	X-ray	7.6	0.32	0.992
	Planar orientation			
	thickness: 20 μm	8.9	0.34	0.992
	150 μm	7.8	0.42	0.976
	Homeotropic orientation	11	0.44	0.84
OOBAMBMC	X-ray	6.8	0.38	0.993
OOBAMBCC	X-ray	7.9	0.31	0.998
TDOBAMBCC	X-ray	6.75	0.40	0.989
	Planar orientation			
	thickness: 150 μm	6.0	0.27	0.98
	20 μm	5.3	0.33	0.96
	Homeotropic orientation	7.7	0.31	0.98
DOBAMBCC	Planar	6.6	0.40	0.975
HOBACPC	Planar	5.6	0.43	0.92
	Homeotropic	6.6	0.37	0.8

For θ_o the values obtained are quite similar for the four compounds, taking into account the experimental dispersion of the data. At this point, it seems more realistic to make a single fit on all the data. This global fit is shown on Figure 3 as a continuous line. It corresponds to $\theta_o = 7.3^\circ$, $\beta = 0.35$ and $r^2 = 0.975$. The critical exponent β is exactly the one predicted by the theory using the renormalization group technique,⁷ for the case of an order parameter of dimension 2 and a space dimension 3, corresponding to the smectic C* case. However, this β determination may be questionable, because the range of temperature is of only one decade. Moreover, we suspect a systematic error on the temperature scale in this experiment: the data accumulation takes about one hour for each point. Because T_c shifts of about one degree for 24 hours, this results in a possible shift of the order of one degree for the largest ΔT points. The effect of this shift is to decrease β ; a corrected value would give β closer to 0.4, as shown also by the best value of r^2 . The value 0.4 compares well with what has been obtained on the tilt of DOBAMBC by Ostrowsky *et al.*⁹ and more generally on non chiral smectic C by Galerne.¹⁰

Optical measurements of the tilt angle

The problem is to measure the tilt angle of the main axis of the optical dielectric tensor. In principle, this is possible by observing the helicoidal texture of a chiral C* normally to its axis, as explained by one of us.¹¹ Practically for sys-

tematic measurements, we found more accurate to proceed differently, by measuring the tilt after the helix unwinding. According to the planar or homeotropic sample orientation, we use two different methods.

a) Optical tilt measured in planar geometry

We use the planar geometry described in the Section III devoted to pitch measurements. We apply a strong enough electric field to unwind the helix, as explained later in the Section IV devoted to polarization measurement. We assume then that the uniform texture obtained is the one of an ordinary C phase i.e.: the molecules are all parallel, parallel to the plates and tilted across the normal to the layers by the tilt angle θ . The neutral lines of the sample slab give the two axis of the optical tensor. The tilt θ is obviously the angle between the largest axis and the rubbing direction, which gives the molecular direction in the smectic A phase.

In practice, we find convenient to place the sample on a rotating stage between two crossed polarizers (Figure 10). We apply a DC field across the sample above the unwinding threshold field with one given polarity. We determine the position of the stage for extinction. We now reverse the field polarity, keeping the same field amplitude. The angle of rotation of the stage to reobtain a complete extinction is 2θ . On the average for good samples, we find large areas where the extinction is quite uniform. The tilt values are quite reproducible for $150\text{ }\mu\text{m}$ samples. The behavior of thin samples ($10\text{--}20\text{ }\mu\text{m}$, comparable to the pitch) is particular and will be described later.

To obtain the planar geometry, the sample is placed between two rubbed glass plates. In the A phase, the texture is uniform. In the C phase (the unwound C*), there must be a transition layer close to the plates, where the mean molecular orientation turns to adjust to the bulk tilted orientation. (This implies the assumption that the layers do not move from the S_A to the S_C phase; an experimental check of this assumption is the absence of motion of defects, or focal conics, at the transition). We assume that the thickness of the transition layer is small enough so that the optical properties of the sample are the one of the uniform bulk texture.

We find that the position of the stage for complete extinction does not depend on the field amplitude even with a field ten times higher than the critical field. From this observation, we can deduce that θ is quite the same in the helical as in the unwound texture and that the transition layer has probably a very small influence on the measurement.

On Figure 4 we have plotted our θ measurements for the DOBAMBC in three conditions: first we cool slowly the sample from T_c down to the C* phase; second we heat slowly to go back into the A phase; third after five days in the A phase we go down again through the C* phase.

The first point to observe is the large hysteresis between the two first curves, although the points have been measured in about one hour to minimize the

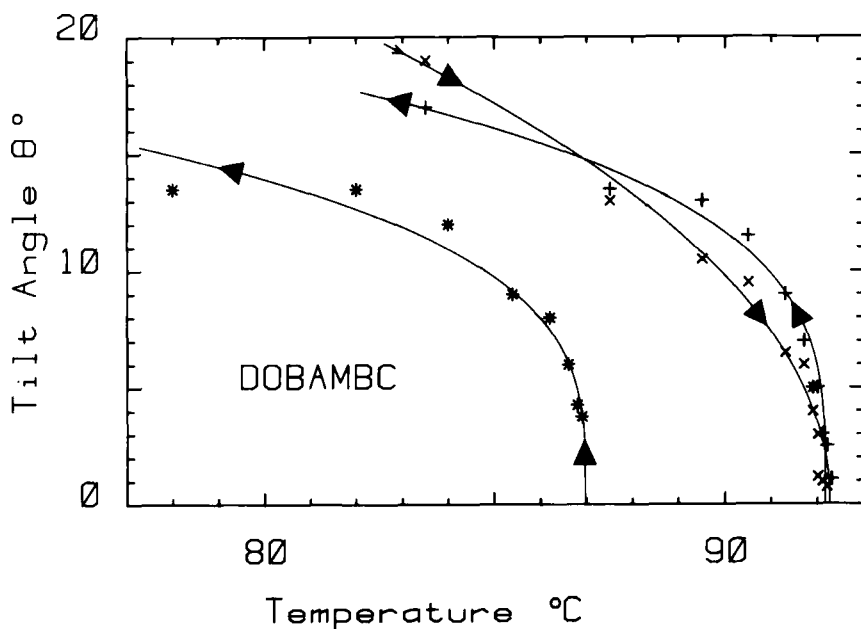


FIGURE 4 Tilt angle versus temperature, from optical measurements in planar geometry. Crosses: hysteresis effect. Star: same data after 5 days aging in the C phase, showing the T_c down shift.

shift of T_c which is in the order of the accuracy of the temperature measurements ($\pm 0.1^\circ\text{C}$). That hysteresis on θ is larger than the optical angular accuracy ($\pm 0.5^\circ$). We believe this hysteresis to be a mechanical one related to an irreversible distortion of the transition layer near the boundaries.

The second point is the large down shift (5°C) of T_c after five days. Fitting the curves one and three (corresponding to points obtained by cooling) on a power law $\theta = \theta_o(T_c - T)^\beta$ gives $\theta_o = 6.6^\circ$ and 8.05° and $\beta = 0.48$ and 0.28 respectively. The compound degradation changes both the transition temperature and the apparent critical exponent. To obtain more reliable results, we have accumulated the measurements of three new samples (Figure 5). A global fit of these data (see Table II) for DOBAMBC, gives $\theta_o = 7.8^\circ$ and $\beta = 0.42$.

We have plotted on Figures 6, 7, and 8 the tilt measurements of three other compounds, the HOBACPC, DOBAMBCC and the TDOBAMBCC. The corresponding fitted values are shown on Table II. These results will be discussed later, in comparison with those obtained with the homeotropic technique.

Case of thin samples

An interesting observation on TDOBAMBCC in the planar geometry is that the temperature at which a spontaneous twist occurs (in absence of field) de-

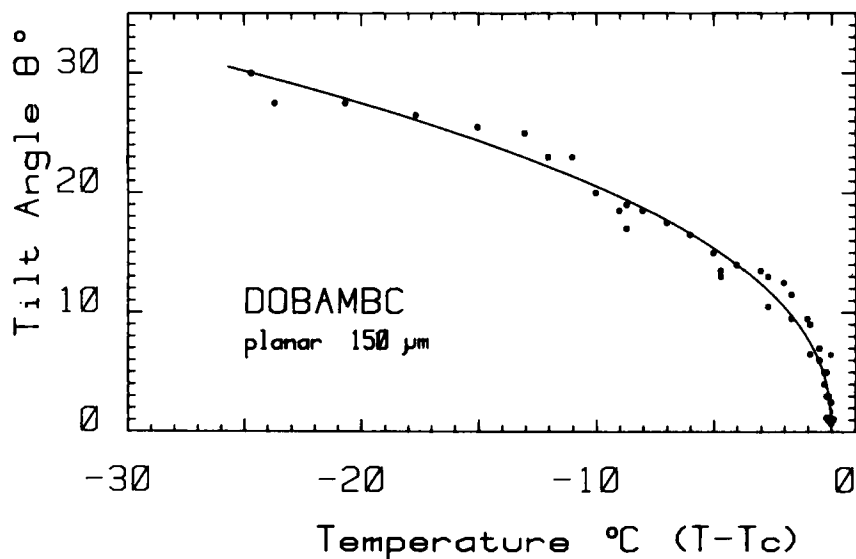


FIGURE 5 Tilt angle from 4 compounds, versus reduced temperature. The continuous line is the best fit (see text).

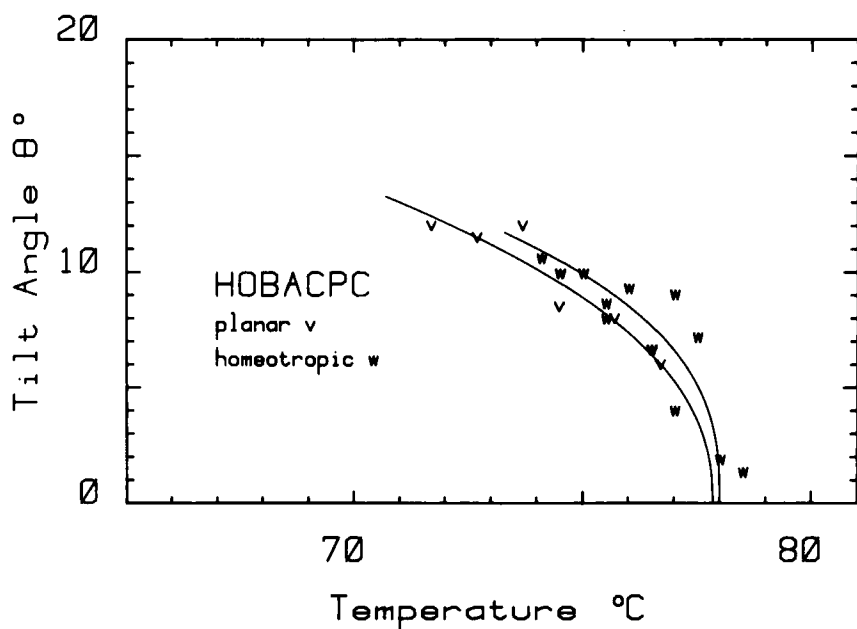


FIGURE 6 Optical tilt versus temperature for HOBACPC.

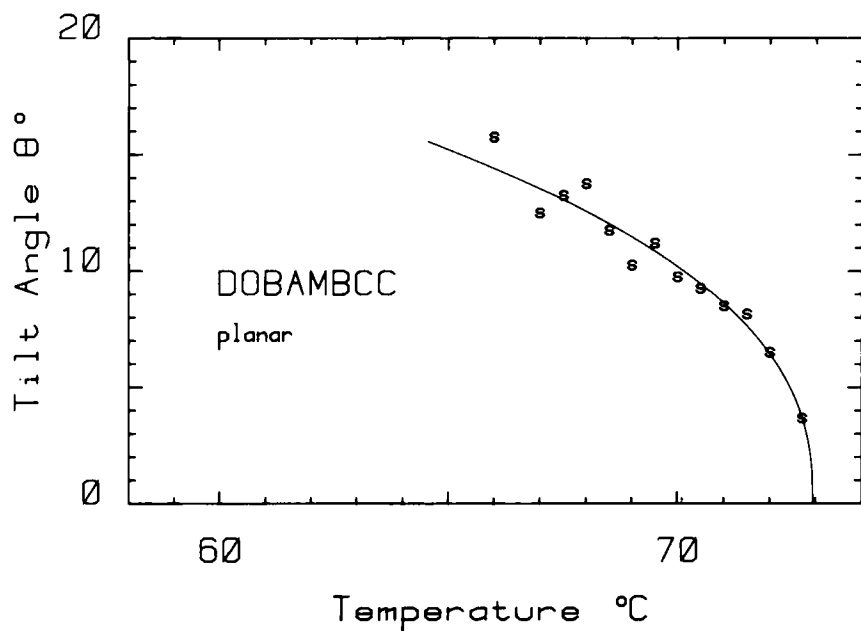


FIGURE 7 Optical tilt versus temperature for DOBAMBCC.

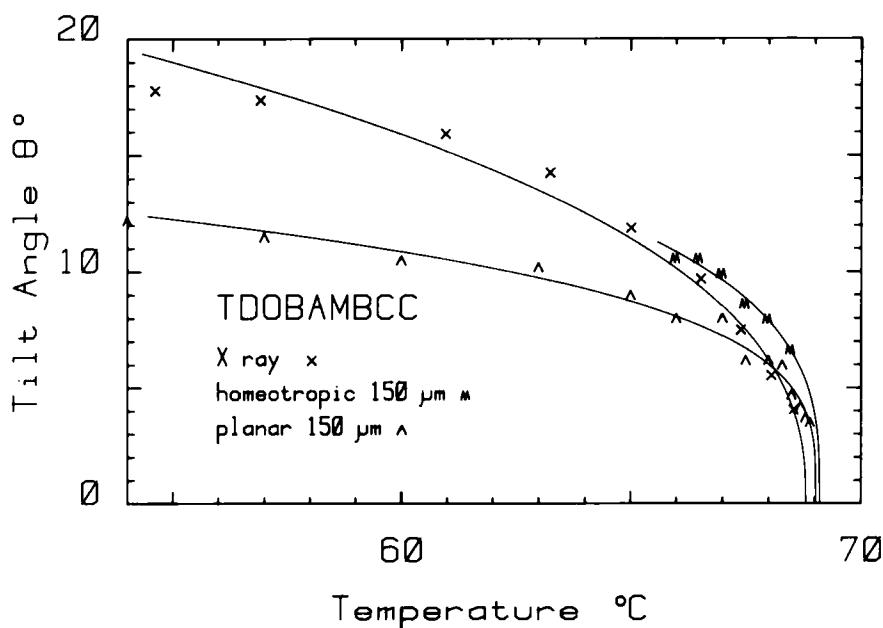


FIGURE 8 Optical and X-rays tilt versus temperature for TDOBAMBCC.

crease strongly for small thickness samples. When cooling a thin sample from the S_A to the S_C phase, one first observes at a temperature lower than T_c the appearance of small colored iridescent regions, then, at an even lower temperature, the periodic striations characteristic of the helical texture. Heating back, the striations remain visible up to T_c . The corresponding temperatures are plotted on Figure 9 versus the sample thickness. The apparent T_c decrease, which can be quite large (more than 15°C down shift for a $20\text{ }\mu\text{m}$ thickness) can be understood as due to the competition between the spontaneous twist and the orientation quenching from the plates in presence of strong anchoring. Calling d the sample thickness, the nematic Frank energy per unit volume necessary to adjust the untwisted texture to the plates goes as $K\theta^2/d^2$. The energy gained by the spontaneous twist process compared to the uniform texture goes as $K_o\theta^2q_o^2$, where q_o is the spontaneous helical torsion. For the helical texture to appear, one needs the condition $K_o\theta^2q_o^2 > K\theta^2/d^2$, i.e.

$$q_o d > (K/K_o)^{1/2} \sim 1$$

The pitch should be smaller than the sample thickness. The observed apparent T_c shift follows roughly the temperature variation of the pitch observed for this sample (see Section III). A question remains: what is the nature of the domains observed in the temperature range between the appearance of iridescence down to the appearance of striations? We first note that these domains remain visible at lower temperature, superimposed on the helical striations. Observed between crossed polarizers, these domains appear as regions where

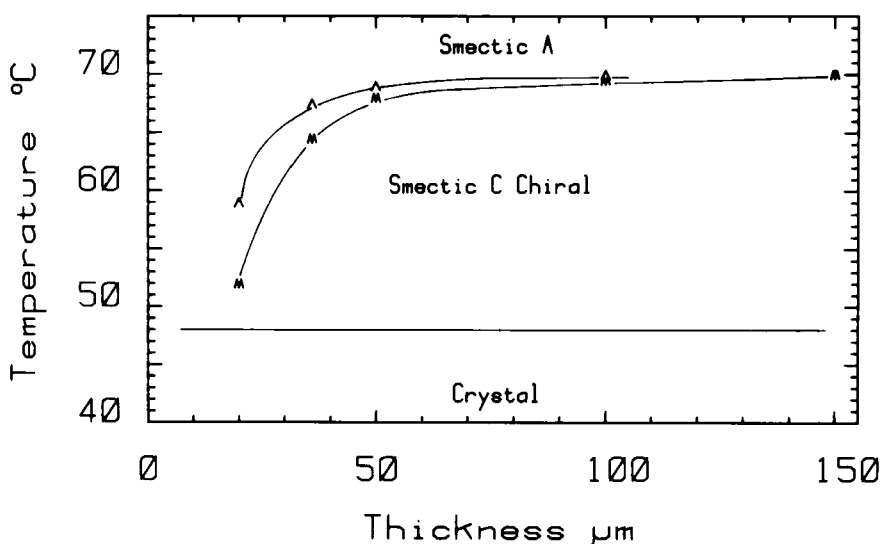


FIGURE 9 Apparent T_c down shift versus sample thickness. Δ : appearance of iridescence. M: appearance of the striped texture.

the molecular orientation is rotated compared to the field of observation. The domains can be erased by the application of an electric field. We observe two kinds of domains, the one sensitive to a DC field in one direction, the other sensitive to the opposite direction. We understand these domains as resulting from a local uncontrolled surface anchoring.

b) Optical measurements in homeotropic geometry

As usual in all this paper, we call homeotropic the smectic C* texture obtained by cooling an homeotropic smectic A texture, i.e. a texture where the smectic layers are parallel to the boundaries glass plates. The helical axis of the C* phase is then perpendicular to the plates. To obtain the homeotropic alignment in the A phase, we use the usual silane coating on the glass plates to force the molecule to align perpendicular to the boundaries. The assumption of the smectic layers parallel to the plates is obviously more appropriate in this geometry than the perpendicular assumption in the planar geometry. Here the junction layer necessary to adjust the molecular orientation from the boundary to the bulk is known to have a thickness of the order of molecular dimension. No visible optical effect is expected from such a thin junction layer.

The principle of the tilt measurement in this geometry is the following: the helix is unwound by applying an electric field larger than the threshold field, (see later, Section IV) and parallel to the plates. For large electric field an uniform texture is obtained with the molecules perpendicular to the field and tilted by the angle θ compared to the plates normal (Figure 10). The observed tilt angle is obviously the tilt of the long axis of the optical dielectric tensor. The tilt is measured using the polarized light interferometric conoscopic technique.

We use the experimental setup represented on Figure 10. An He-Ne laser beam linearly polarized is focused inside the sample by a microscope lens (Leitz UMK 32). The width of the laser beam is adjusted to cover the maximum angular aperture of the lens (0.2). At the output, this conical beam passes through a linear analyzer crossed with the polarizer. The light is observed on a screen which can be rotated around an axis parallel to the plates and passing through the sample. Centering the screen on the conoscopic figure by this rotation allows a measurement of the tilt. The distance of the screen to the axis is large compared to the sample thickness (40 mm compared to 10 μm), and the size of the focused region (a few μm), so that we obtain on the screen the same conoscopic figure as at infinity.

The sample is prepared between two squared glass plates (1 cm \times 1 cm) coated with a silane (Dow Chemical XY 22 300) polymerized at 100°C in a N₂ atmosphere for about one hour. To apply the electric field parallel to the plates and the axis of rotation of the observation screen, we use as electrodes two stainless steel strips of various thickness (to match with the variable sam-

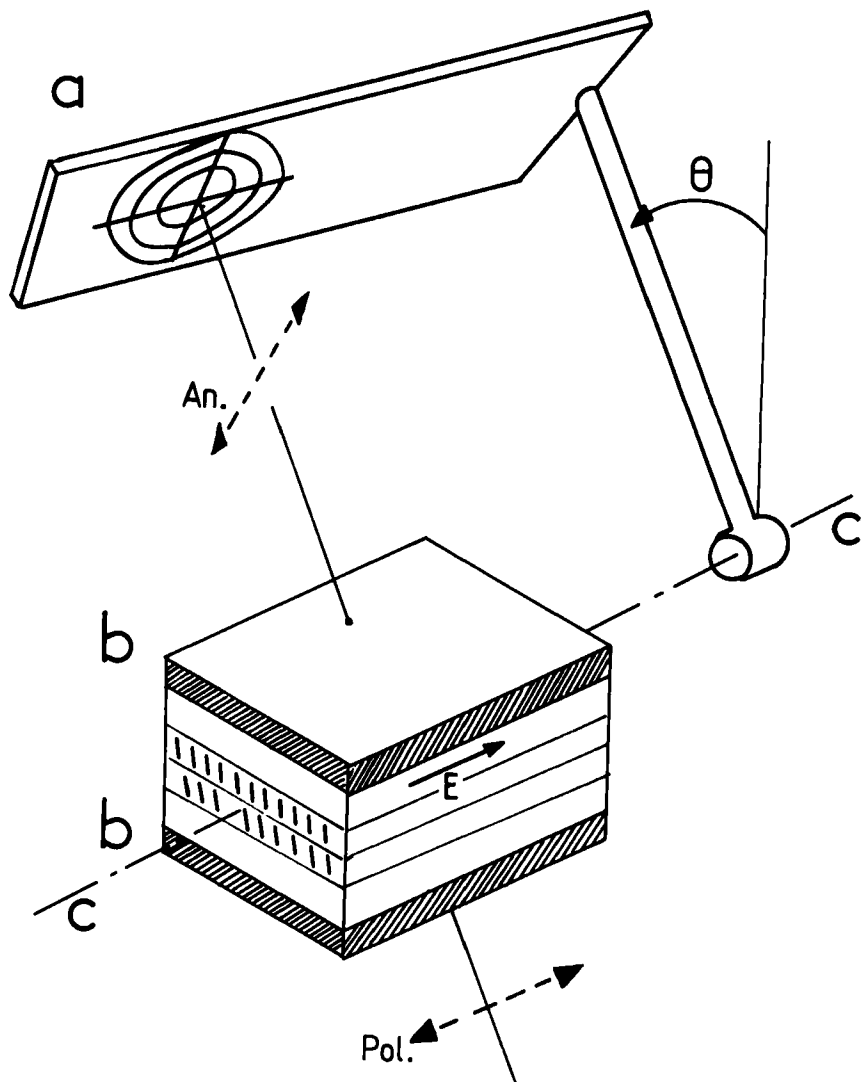


FIGURE 10 Geometry of the conoscopic experiment. a: tilted observation screen. b: silane coated glass plates. c: rotation axis for the screen. E: electric field orientation.

ple thickness from 50 to 500 μm). These two strips are parallel and separated by about 2 mm. The sample is placed in an electric oven of adjustable temperature. The oven temperature is electrically regulated, within 0.1°C. The sample cell is filled in the isotropic phase by capillarity. The rapid cooling to the smectic A phase induces in general the homeotropic alignment, although some thermal cycles back to the isotropic phase are sometimes useful to improve the

sample quality. One can check optically the quality of the homeotropic texture with the conoscopic setup, which allows the choice of the best part of the sample. A severe limitation of our set up is the maximum visible tilt angle in the air, which should not exceed 10° of angle, because of the geometry of the oven.

We first describe what we observe on a typical sample. In the A phase, we observe the usual conoscopic image constituted by a black cross and a series of concentric rings. This pattern is centered around the normal to the sample plates. This is a criterium of a good homeotropic molecular orientation.

We now cool slowly the sample in the C* phase. The observed conoscopic image remains centered. We just observe that the rings become broader and less contrasted. In the center of the black cross, we can now see some light, linearly polarized and turned by a few degrees from the incoming polarization. This pattern is quite similar to the one observed along the C axis of quartz. We understand this pattern, as an averaging effect in the helical texture. The helix cannot force the light polarization to follow the pitch. In all the directions excepted the one of the helical axis, a birefringence averaged by the helix is obtained. In the direction of the axis of the helix, this averaging gives no birefringence but a small rotatory power typical of the C* phase.

We now apply an electric field at 45° with respect to the polarizer. We observe that the pattern tilts linearly in field, in the direction perpendicular to the electric field (Figures 11 and 12). Above a given field threshold, the pattern is destroyed and rebuilds itself slowly with a new axis slightly more tilted than

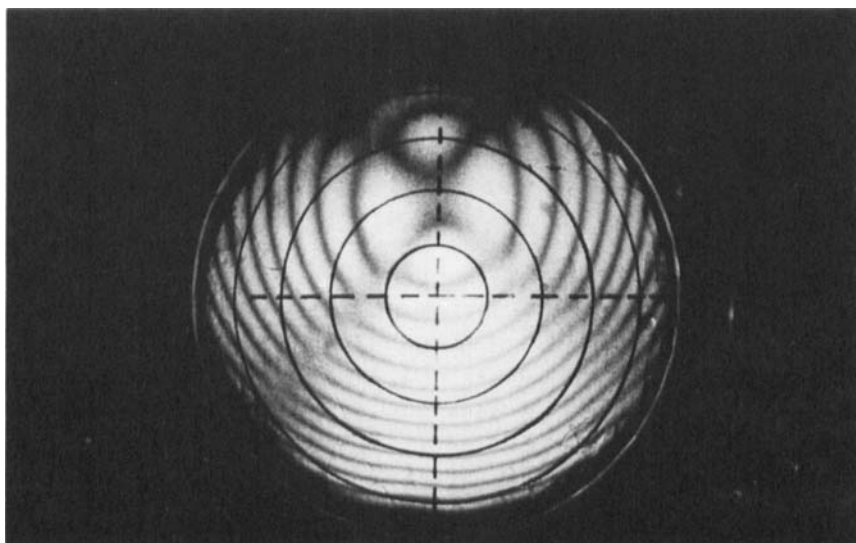


FIGURE 11 Conoscopic picture from the unwound C* phase. The polarizer and analyzer are rotated by 45° compared to E.

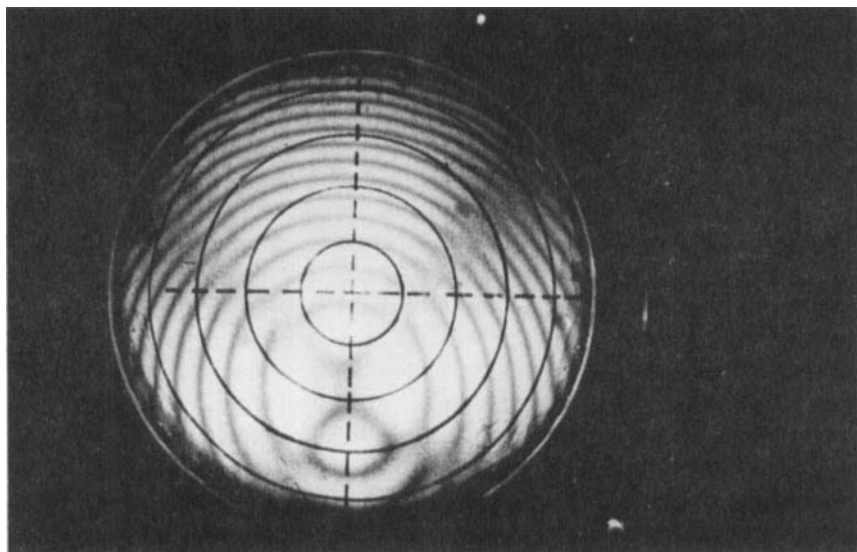


FIGURE 12 Same as Figure 11, with the opposite electric field $-E$.

previously. This pattern does not show any indication of rotary power. It looks like the one of a typical non chiral smectic C.

We measure the tilt angle, in the air (after refraction), of the center of the conoscopic pattern, versus the temperature. To derive the molecular tilt, we take into account the refraction using as ordinary refractive index the value 1.55 for all the compounds. Our reduced data for the tilt are shown on Figures 13, 8 and 6 respectively for DOBAMBC, TDOBAMBCC and HOBACPC. Our best data are obtained for DOBAMBC, on Figure 13. Note that the temperature range has been restricted to 2°C close to T_o to keep the tilt angle in the range allowed by the oven geometry. Our data can be fitted on a power law $\theta = \theta_o(T_c - T)^\beta$ with $\theta_o = 11^\circ$ and $\beta = 0.44$.

This fit is shown in solid line. For comparison, we have plotted the fit on X-ray data for this compound, and the fit on the tilt observed in planar geometry. Within our experimental uncertainty, in the range of 2°C , the X-ray and optical planar data look similar, but both are significantly smaller than the optical homeotropic data. We do not believe that the uncertainty on the refractive index can explain this discrepancy. Note in addition that at lower temperature, the large difference in the exponent β (0.32 and 0.42) makes also a significative difference between X-rays and planar data.

On Figure 8, we have plotted all our tilt angle data for TDOBAMBCC. Here, we find that, close to T_o , the homeotropic data seem to agree reasonably with X-rays, although for large temperature shift, we observe a significative difference between X-ray and planar data. In opposition with the case of

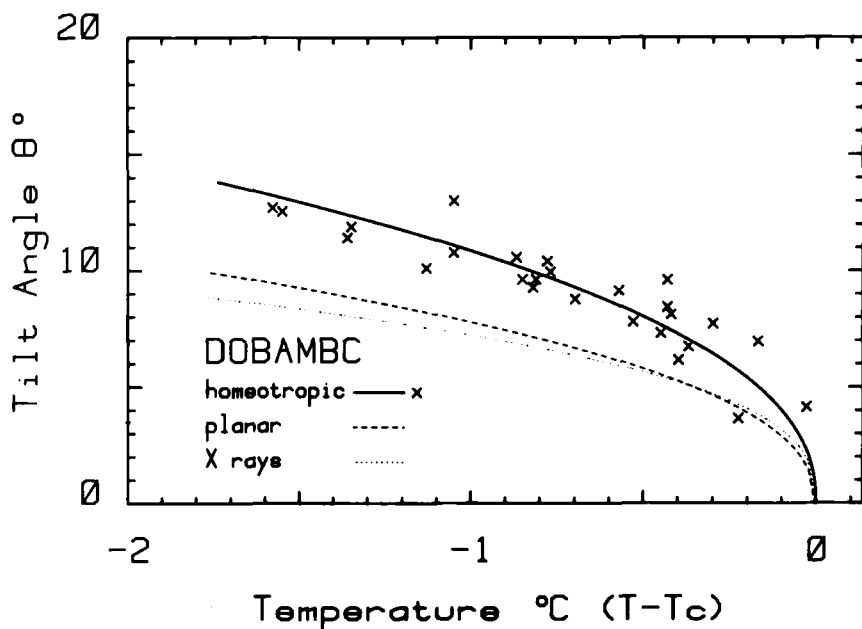


FIGURE 13 Comparison between optical and X-ray tilts versus reduced temperature close to T_c for DOBAMBC.

DOBAMBC, the X-ray tilt angles are here 50% larger than the planar ones, although they are 30% smaller for DOBAMBC.

Our last data, for HOBACPC (Figure 6), seem to indicate a relatively good agreement between planar and homeotropic values, and also with the averaged X-ray data. However the larger uncertainty of the data prevents any more definite conclusion.

To summarize, we have observed X-ray tilt angles which seem very comparable for all measured compounds, and optical tilt angles which are sometimes significantly different, depending on the observation geometry. We are not disturbed by the difference between X-ray and optical measurements. We know⁶ that our rigid rod model is questionable, especially for the compounds with long (and flexible) aliphatic tails, as for instance TDOBAMBC. On the other hand, comparing only optical data, we observe that the tilt angle measured in homeotropic geometry is always larger than the one deduced from planar geometry. We can explain this systematic difference by the uncontrolled junction layer in planar geometry which results always in an apparent lower tilt angle. Our conclusion is that the homeotropic method is more correct for the tilt angle determination. Unfortunately, our data are restricted to a small range of temperature. It would be interesting to design a better experimental setup to extend the range of tilt angle available.

To conclude this section, it is useful to indicate the sign of the molecular tilt compared to \mathbf{P} in the unwound texture. All the compounds were synthesized from the same chiral ester. Those possessing a cyano group have their molecules tilted in one direction, all the other in the opposite, as shown in Figure 14.

III PITCH MEASUREMENT OF THE HELICAL TEXTURE

The pitch Z of the helical texture of the chiral smectic-C is an important parameter in all experiments in which the twist energy of the texture is implied. In a planar geometry, the helix results in a striped texture.^{2,11} The spatial period L of the stripes is obviously related to Z . We discuss first how we connect L and Z . We then present our pitch measurements for 6 chiral C* compounds of Table I.

To measure the pitch we use C* samples oriented in the planar geometry (Figure 15) i.e. samples obtained in C* phase by cooling a planar smectic A sample, keeping the smectic layers normal to the glass plates. In practice, to obtain this alignment we use two standard NESA tin oxide coated glass plates with a second coating of oblique evaporated SiO imposing a molecular alignment parallel to the plates,¹² and perpendicular to the evaporation direction. These plates are separated by mylar or glass spacers. In order to regulate the sample temperature up to 0.1°C, the liquid crystal cell is placed in a Mettler

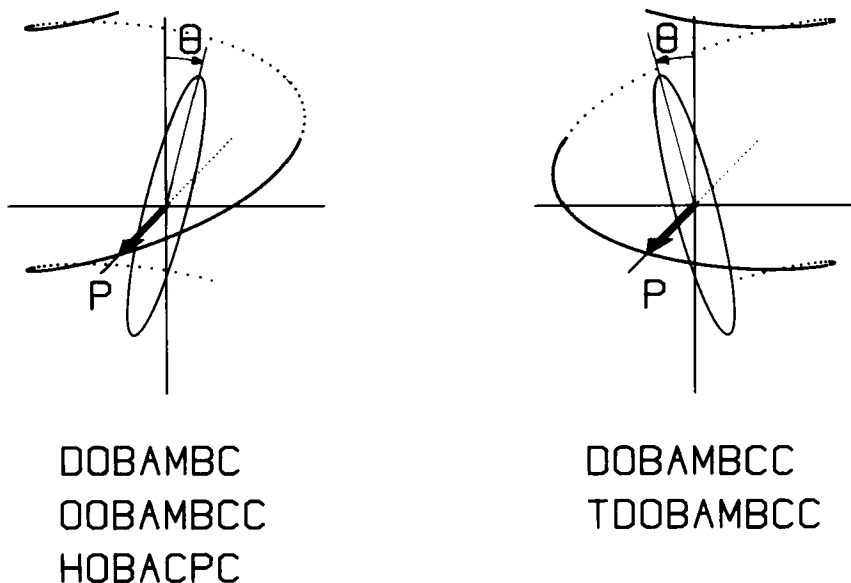


FIGURE 14 Relative orientation of \mathbf{P} and θ for the five studied compounds.

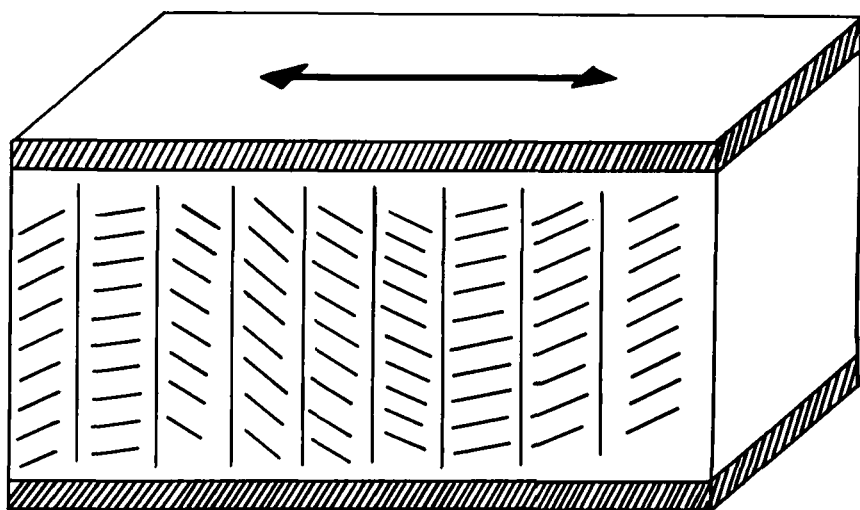


FIGURE 15 Planar geometry. The arrow indicates the rubbing direction on the upper and lower obliquely SiO evaporated plates.

hot stage. The tin oxide coating is used as an electrode to apply an electric field normal to the plates.

The compound is inserted in the cell by capillarity in the isotropic phase. A slow cooling down to the smectic A phase gives the planar alignment of the molecules. The application of an AC electric field of less than 10 V/cm at 20 Hz during the slow cooling is sometimes helpful. The sample is observed with a Leitz polarizing microscope having a graduated circular turn table and a micrometer in one of its eye pieces.

How can we derive the pitch of the helix from the stripe spacing? Why the problem arises is obvious from Figure 16 which represents photograph of chiral C* samples in non uniform texture. This picture shows that the texture is a focal conic arrangement, in which we can see the stripes perpendicular to the axis of the helix. Stripe spacing on this figure is not exactly representative of the pitch, for two reasons: first the texture is presumably tilted, resulting in an apparent spacing varying from one place to the other. Second, we do not know if the spacing represents the pitch Z , or half the pitch $Z/2$. This point is best understood on Figure 17 which shows an enlarged portion of a transition between two regions where stripes have slightly different directions. It is very apparent that a region of the picture shows a stripe spacing two times larger than the other one. Moreover, changing the focus, one can find back a period two times smaller in the large period region. To suppress the first difficulty, we have made stripe spacing measurements on planar samples of reasonable quality (Figure 18). Now we need a criterion to define the pitch. We have found such a criterion by applying a DC or AC electric field E on the sample,

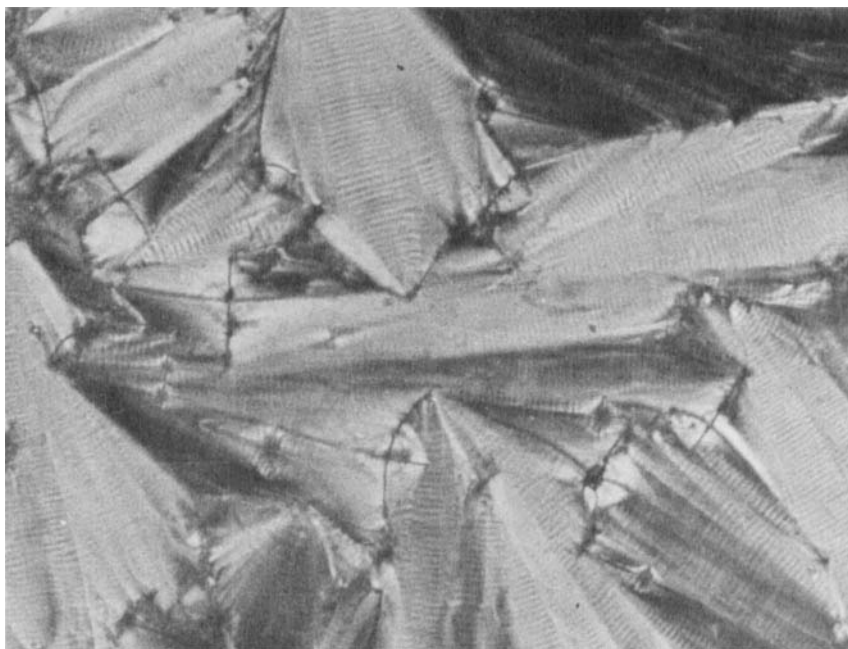


FIGURE 16 Chiral C^* polydomain texture showing focal conic arrangements.



FIGURE 17 Enlarged area from picture 16, showing the double spatial periodicity associated with the half pitch $Z/2$ of the helix.

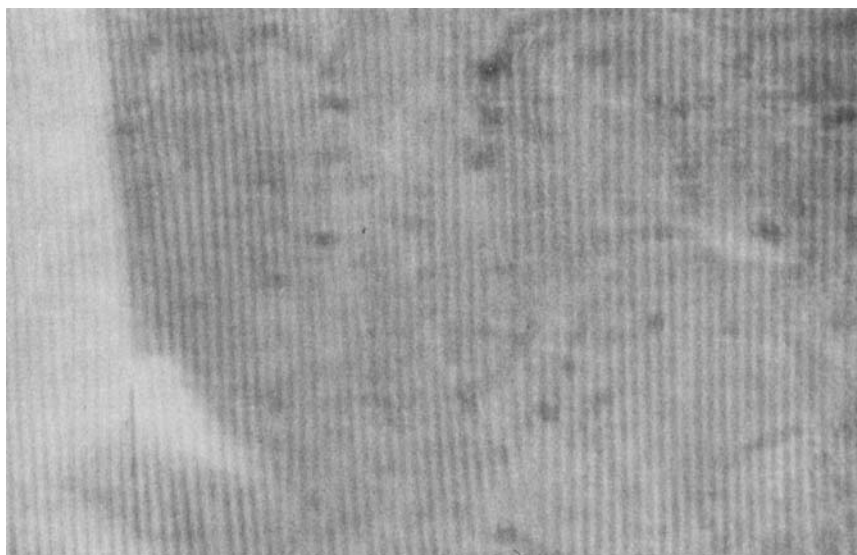


FIGURE 18 Picture of a well aligned planar sample.

perpendicular to the plates. There is a critical field which unwinds the helix. In some samples we have observed that, close to the critical field, the stripe spacing increases, as in the cholesteric to nematic unwinding. In very good samples, as in Figure 18, the stripes spacing remains uniform when E increases, especially with an AC field. In most samples with a DC field, the stripe spacing increases by the local disappearance of one (or more) stripes. The Figure 19 shows examples of these stripes isolated in a uniform alignment region. This figure must be compared to Figure 20 representing the same sample without applied E field. Adjusting the field slightly makes these isolated stripes move forward or backward. The topology of these isolated stripes imposes that the texture inside is a conical twist characteristic of the C^* , of one (or an integer number of) turn around the helical axis. The optical appearance of each stripe, composed of a succession of black, white, and black regions, confirms that there is only one turn in the isolated stripe. Going down now to zero E field, we observe that the helix is formed by the melting of adjacent black sides of neighboring stripes. We conclude that the stripe spacing L in most planar textures is equal to the pitch Z . This is also confirmed by the observation in uniform planar textures of stripes dislocations. These dislocations should also represent a jump of an integer times the pitch; their presence (as in Figure 21 for instance) is a criterion of the line spacing.

Using the criterion defined in the previous section, we have measured the pitch versus temperature for 6 compounds presenting a C^* phase. A difficulty

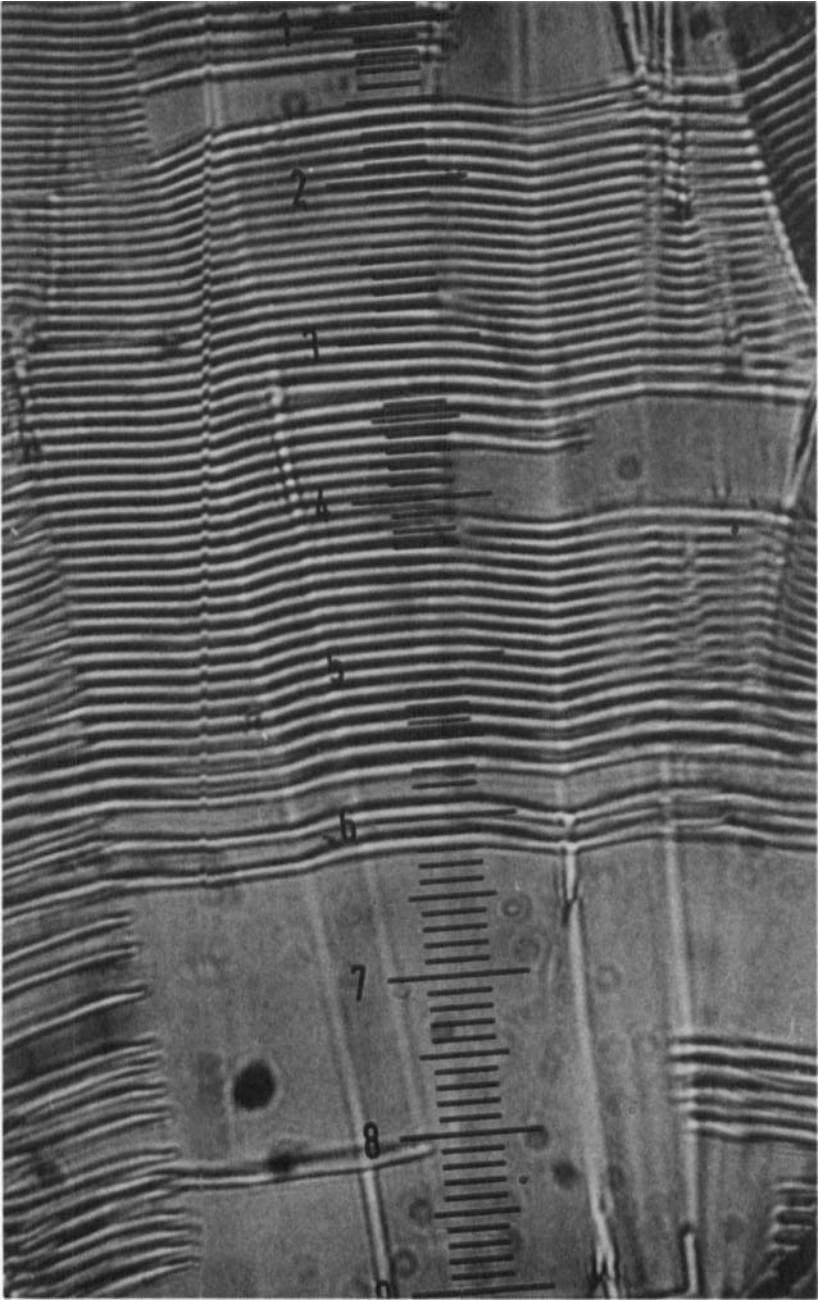


FIGURE 19 Picture of a partially unwound sample by a DC electric field close to threshold.

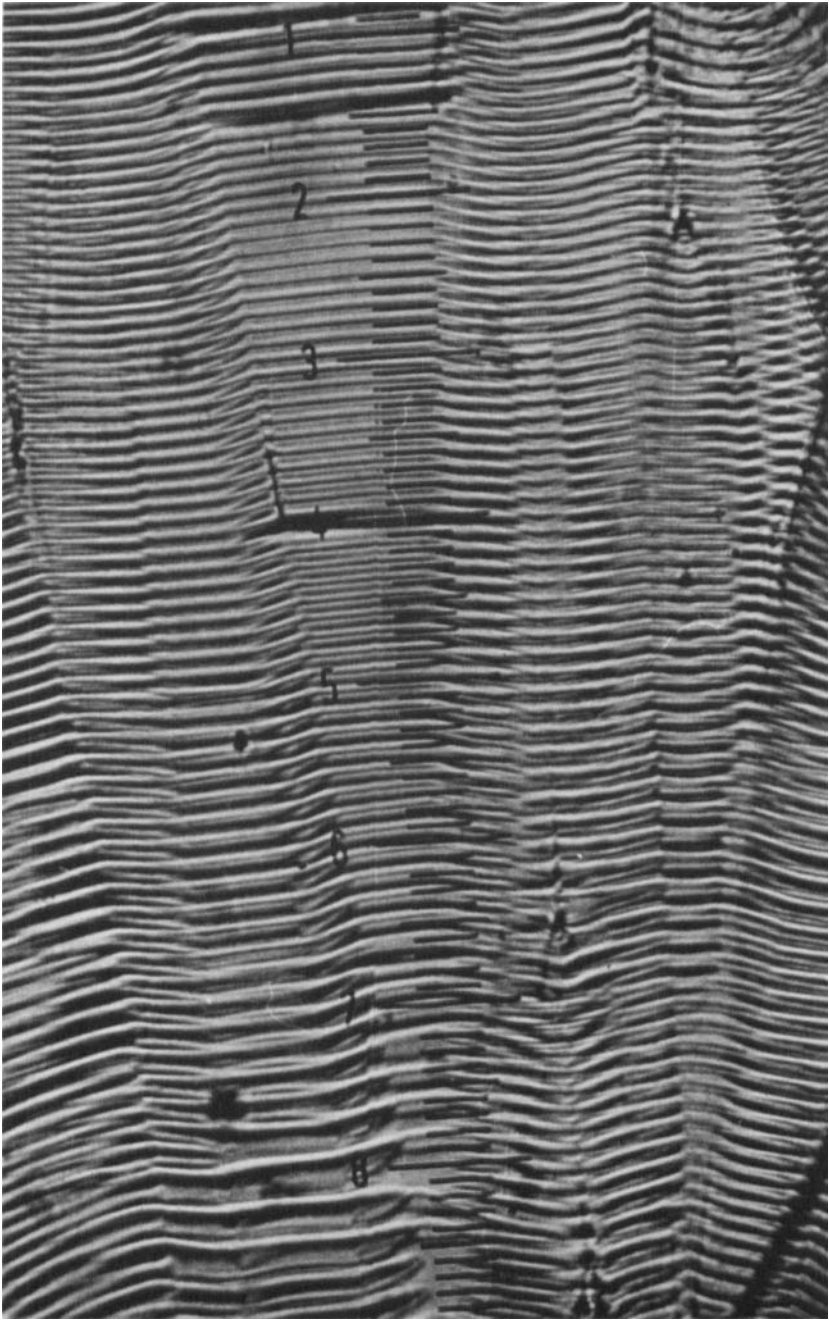


FIGURE 20 Same sample as on Figure 19, in absence of electric field.

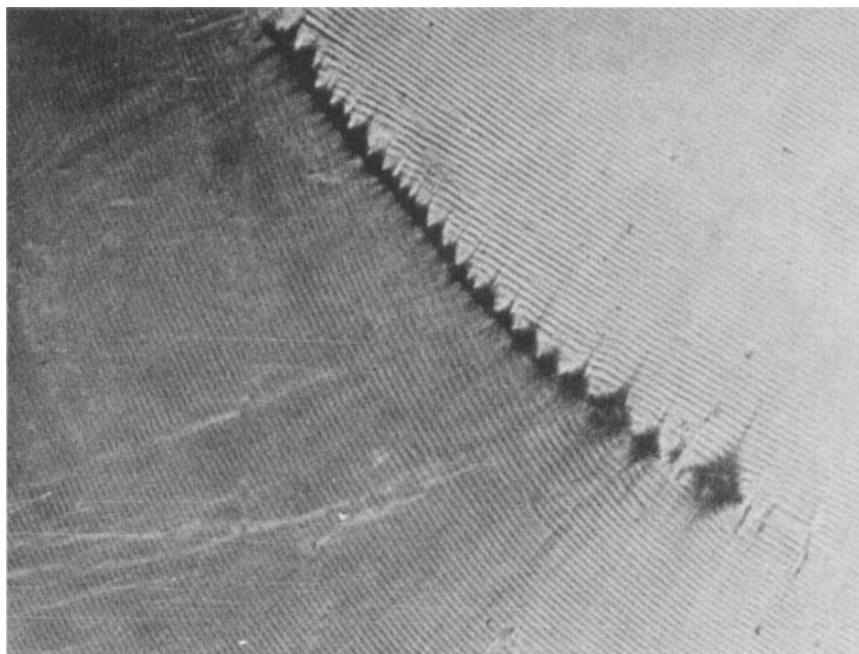


FIGURE 21 Domain separation between two uniformly oriented planar regions, of slightly different alignment. One can see dislocations of the stripes.

of these measurements is to be sure that the observed pitch has taken its equilibrium value. In fact, we have found that, when not using any electric field, some compounds seem to show a pitch constant when the temperature is changed. The application of a DC electric field above threshold unwinds the helix. Turning off the field lets the helix to rewind, with a value of the pitch hopefully closer to its equilibrium value. A typical behavior of this sort is shown on Figure 22 for the TDOBAMBCC which shows an increase of Z close to the transition temperature. One sees distinctly the difference between data taken without applying any electric field (stars), and the data in presence of an electric field (open triangles). The pitch Z seems to decrease generally with decreasing temperature; close to T_c significant values of Z imply the use of the electric field. We observe that the pitch seems to decrease sharply close to T_c . We cannot be sure experimentally that Z decreases down to 0. In fact, close to T_c , the pitch which is an even function of θ has no reason to vanish. On the other hand, the effect of some chiral molecules, which would not follow the smectic ordering, is not expected to decrease. As the twist elastic constant $K_o\theta^2$ vanishes at T_c , the resulting spurious twist may be quite strong close to T_c . This effect is just the opposite of the one observed in cholesterics close to a lower smectic phase, where the twist constant diverges, giving an increase of the

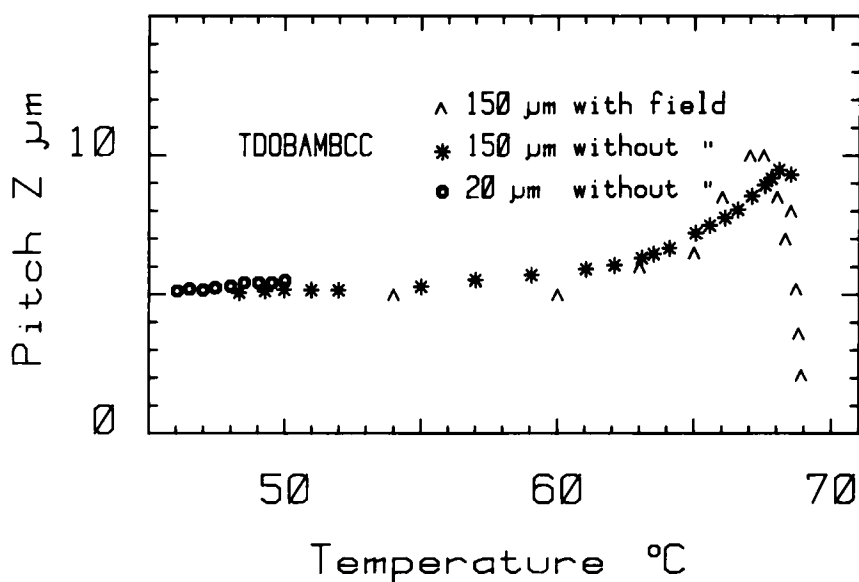


FIGURE 22 Temperature dependence of the pitch of TDOBAMBCC for various sample thickness.

pitch. As the presence of impurities is quite certain in our samples, we remain cautious about the data close to T_c .

We have plotted on Figure 23 all our data for PACMB, DOBAMBC, OOBAMBC, DOBAMBCC, TDOBAMBCC and HOBACPC. The general outlook shows a regular decrease of Z when T decreases. We have not plotted the values close to T_c as explained. The important finding is the peculiar behavior of PACMB which exhibits a diverging pitch at $T_{\infty} = T_c - 4^{\circ}\text{C}$. We have verified that, above and below T_{∞} , the rotatory powers of homeotropic samples of this material are opposite. T_{∞} corresponds to a continuous passage through zero of the twist $q_0 = 2\pi/Z$. Again we are not sure that this effect is intrinsic, it may be due to a balance between intrinsic and impurity induced twist. The largest values of the pitch are limited to about 60 μ , when Z compares to the thickness of the sample.

Taking care of the shape of the experimental data and of the even dependence of Z versus θ we tried to fit the results with an hyperbolic law of the shape $Z = Z_0 + a/(\theta^2 - \theta_a^2)$. All the curves fit reasonably with hyperbolas. The best fits are shown by the full lines on Figure 23 and the corresponding numerical parameter on Table III. We did not find a satisfactory explanation for this law. It is interesting to note the sense of rotation of the helicoidal texture. This sense can be derived from the sense of the rotatory power observed when linearly polarized light propagates along the helical axis. Qualitatively, we find that our compounds can be classified in two groups: the first group contains

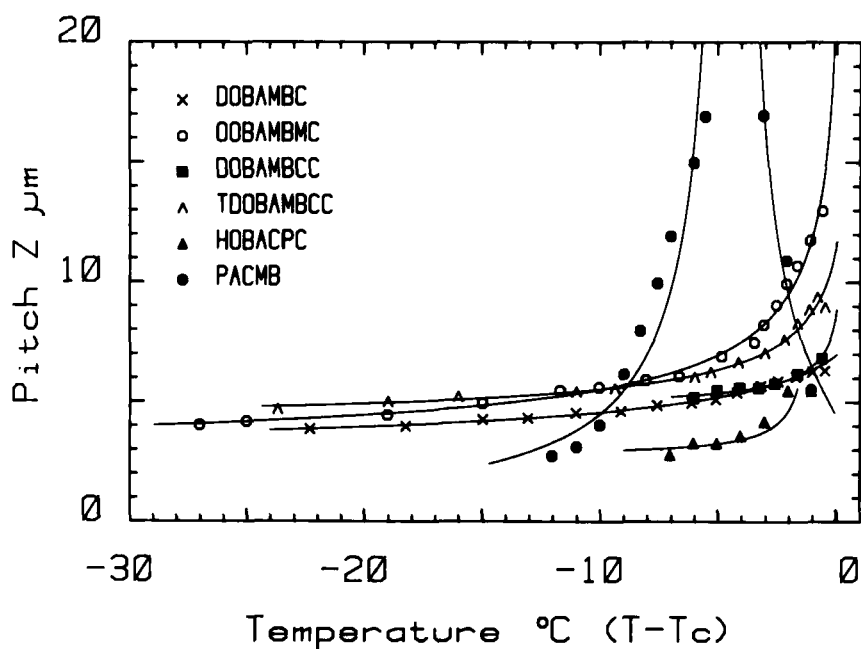


FIGURE 23 Temperature dependence of the pitch Z of the six studied compounds. The continuous lines are the best hyperbolic fit (see text).

TABLE III

Pitch in μm versus tilt angle in degree

$$Z = Z_0 + \frac{a}{\theta^2 - \theta_a^2} \text{ with } \theta = \theta_0 (T_c - T)^\beta$$

$T_c + T_a$ = temperature of divergence of the pitch

Compound	θ_0 and β coming from	a in μm	θ_a	T_a	Z_0 in μm
DOBAMBC	X-ray	1225 ± 40	-215	7.8 ± 0.5	1.94 ± 0.07
	Homeotrope	3076 ± 90	-710	7.5 ± 0.5	2.67 ± 0.05
OOBAMBC	X-ray	921 ± 60	-52.3	1.2 ± 0.3	2.6 ± 0.16
TDOBAMBCC	X-ray	565 ± 35	-65	1.6 ± 0.3	3.9 ± 0.10
	Homeotrope	623 ± 42	-59	1 ± 0.3	3.5 ± 0.16
PACMB	X-ray moyen	572 ± 100	+150	-4.5 ± 0.4	-0.5 ± 1.2
	$\theta_0 = 7.26$ $\beta = 0.35$				
DOBAMBCC	Planar $\theta_0 = 6.6$ $\beta = 0.4$	156 ± 18	-36.4	$+0.8 \pm 0.4$	4.6 ± 0.12
HOBACPC		61 ± 30	28	-0.9 ± 0.8	2.6 ± 0.4

the two nitrile compounds, the TDOBAMBCC and DOBAMBCC. For this group the rotatory power is positive following the convention of optical textbooks. All other compounds have a negative rotatory power. An exception appears, as mentioned, for the symmetrical compound which changes from negative to positive when decreasing the temperature. As the measuring wave length is much smaller than the pitch, in our case of small tilt angle, we can deduce that the mechanical twists are left-handed for TDOMAMBCC and DOBAMBCC and right-handed for the others non cyano compounds.

IV UNWINDING CRITICAL FIELD MEASUREMENT

In presence of a large enough DC electric field transverse to the helical axis, the C* helical texture can be unwound. This comes from the coupling $-\mathbf{EP}$ between the applied field and the spontaneous polarization of the C*. Physically, the critical field E_c can be estimated by balancing the gain in dielectric energy $-\mathbf{EP}$ by the increase of mechanical energy Kq_o^2 , which results in $E_c \sim Kq_o^2/P$. As seen in the first section, K is expected to vary as $K_o\theta^2$ and P as $P_o\theta$. This indicates that E_c should vary as $E_c \sim (K_o\theta q_o^2/P_o)$, i.e. should increase as θ , in a mean field approximation, like $(T_c - T)^{1/2}$. It is interesting to measure E_c versus the temperature, to check this behavior, the parameters θ and q_o being known from our previous measurements. The correct formula for the critical field, given by Meyer,² is $E_c = (\pi^2/16)(Kq_o^2/P) = (\pi^2/16)(K_o\theta q_o^2/P_o)$. A more recent calculation¹³ of E_c has been made, taking into account the coupling of E with the dielectric anisotropy of the material. Up to now, no model is available to describe the behavior in AC field, although the experiment shows that the helix can be unwound by an AC electric field (see below).

Experimental method for planar geometry

We prepare a sample between two glass plates, which are coated to be used as electrodes, as in Section III. We grow a uniform domain sample in planar geometry, using the alignment property of a SiO coating. To generate the DC (and sometimes AC) field, we use a signal generator and a voltage amplifier which allows voltages V up to ± 500 V. The sample thickness is defined by mylar or glass spacers, in the range of 20–200 μm . We define the "applied field" as V/d . We observe the sample, between two cross polarizers, under a microscope.

In absence of field, we see the parallel stripes which visualize the pitch of the helical texture. Applying a large enough DC field makes the stripes to disappear and results in a uniformly aligned smectic C texture in planar orientation. This point is easily verified by the absence of rotatory power and by the fact that, if some defects like focal conics are visible they do not move at all when

the stripes disappear (see Figure 24 to be compared to Figure 20). Decreasing the field, the stripes reappear, with some hysteresis.

Because of this large hysteresis, the determination of the critical field is not easy. In very good samples we take as E_c the mean value of the electrical field necessary to put out the last visible stripe and the field which allows the first stripe to reappear. In less good samples, applying a field makes the stripes to break somewhere and to shrink out of the well aligned parts of the sample, staying into the defects. Lowering the field allows the stripes to grow back with some delay due to viscosity. If we change slowly enough the field amplitude, we can see the stripes moving back and forth without hysteresis. In this case we take as E_c the field which suppresses all the straight parts of the stripes.

In the homeotropic geometry, with the electric field parallel to the plates (see Figure 10), as shown previously in Section II, the complete unwinding of the helical texture is obtained when the ordinary C phase conoscopic figure is visible. At the critical field, unwinding necessitates some time and during this time the screening effect of the ionic charges can lower the field inside the sample. When we increase the field slowly, the conoscopic figure tilts. When it becomes blurred, we keep the field constant noting its value and waiting for the rebuilding of the new black cross. Just after, we decrease the field slowly until the conoscopic figure becomes blurred once again. The same procedure is repeated after changing the polarity of the electric field. The value of E_c is found by taking the average of the above four values.

The critical fields E_c obtained in well aligned samples, using the planar geometry, are shown on Figure 25. They are quite similar for three compounds (DOBAMBC, DOBAMBCC and TDOBAMBCC). E_c increases regularly from zero (close to T_c), to values of the order of 20 stat Volt/Cm for $T_c - T \sim 25^\circ\text{C}$.

It is useful to compare for a given compound the results obtained for E_c in planar and in homeotropic geometry. On Figure 26 are plotted the corresponding E_c values versus temperature for DOBAMBC. Because of the aging of the sample, we observe a large T_c down shift. The points show a relatively large dispersion. The data on planar geometry show a large hysteresis when cooling down or heating the sample, which is probably due to uncontrolled change in anchoring. Screening effect from conduction ions may also occur, varying from sample to sample. For this reason, we trust better the lower valued data, which appear to be the one from the homeotropic geometry. Near T_c , E_c reaches higher values perhaps because of the effect on the pitch of some chiral impurities.

On Figure 27 is plotted for the TDOBAMBCC the E_c results, obtained in the two different homeotropic and planar geometries. Two samples, one in planar geometry and the other in homeotropic geometry, seem to give reasonably well matching data. A third one gives threshold field data smoothly varying in temperature, but larger by a factor 3. We have no certain explanation

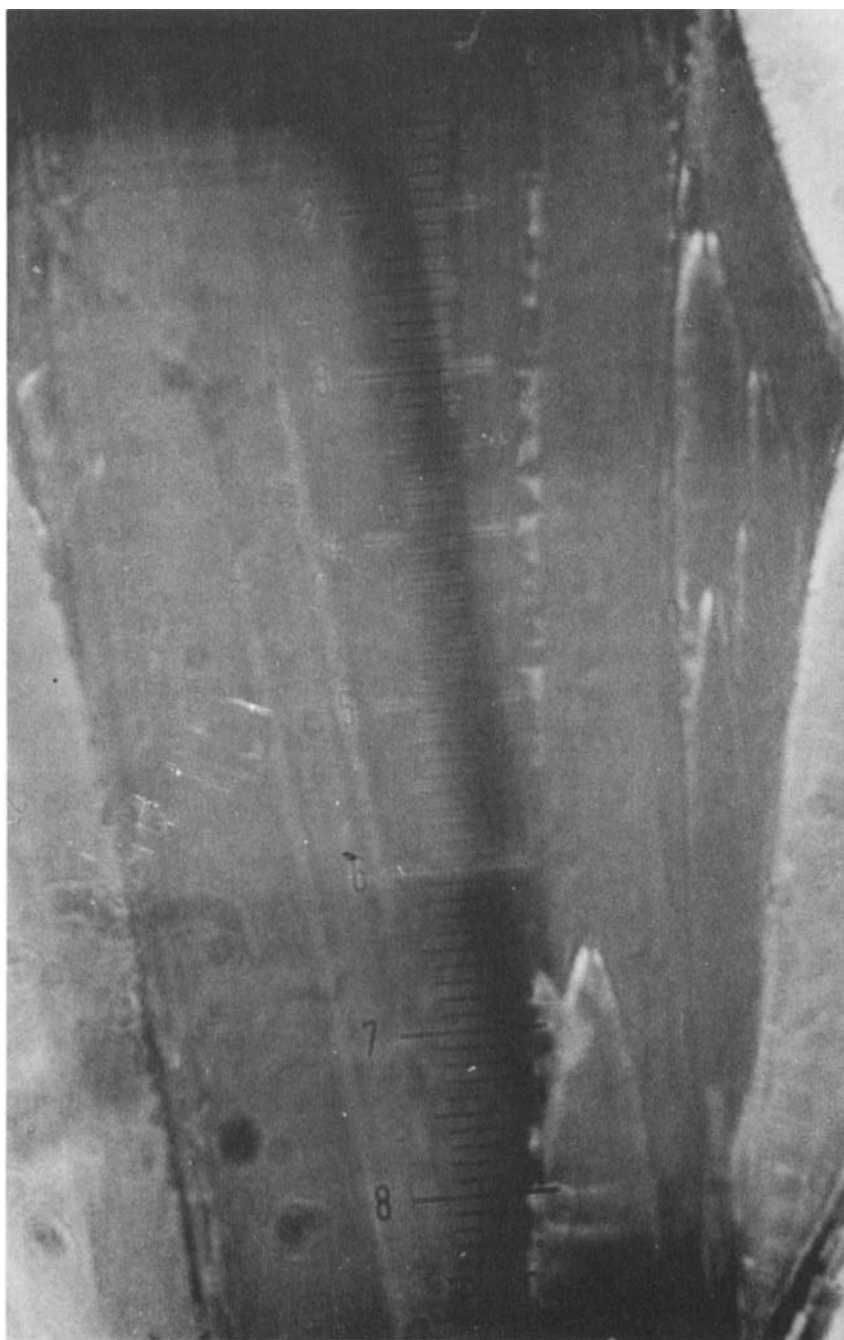


FIGURE 24 Same sample as Figure 19, in the complete unwound state.

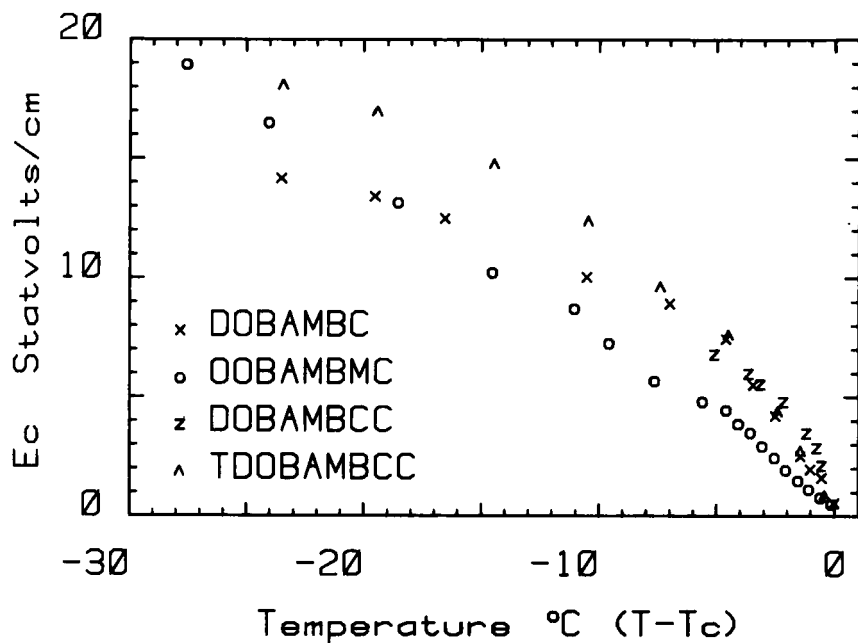


FIGURE 25 Unwinding critical DC field versus reduced temperature for four different compounds.

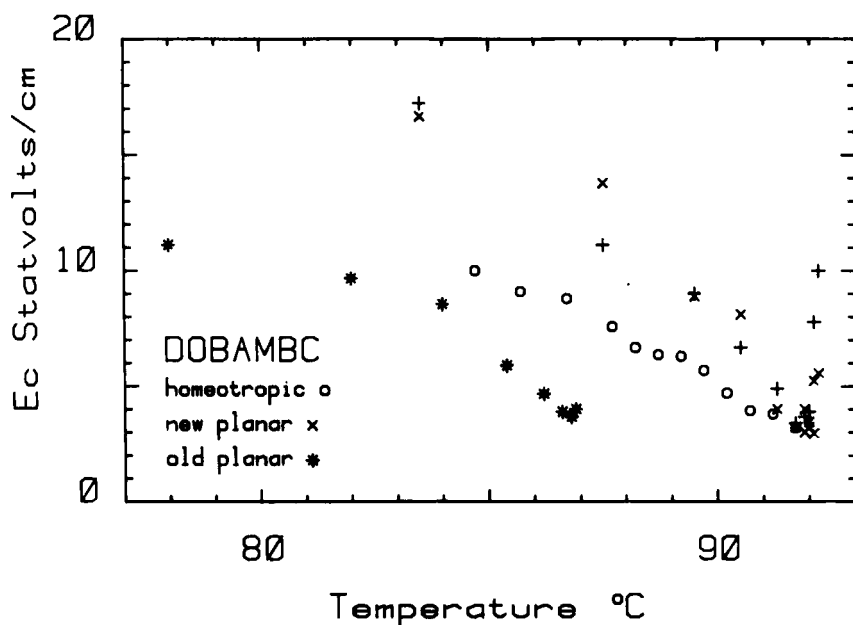


FIGURE 26 Unwinding critical DC field versus temperature for DOBAMBC in various geometries.

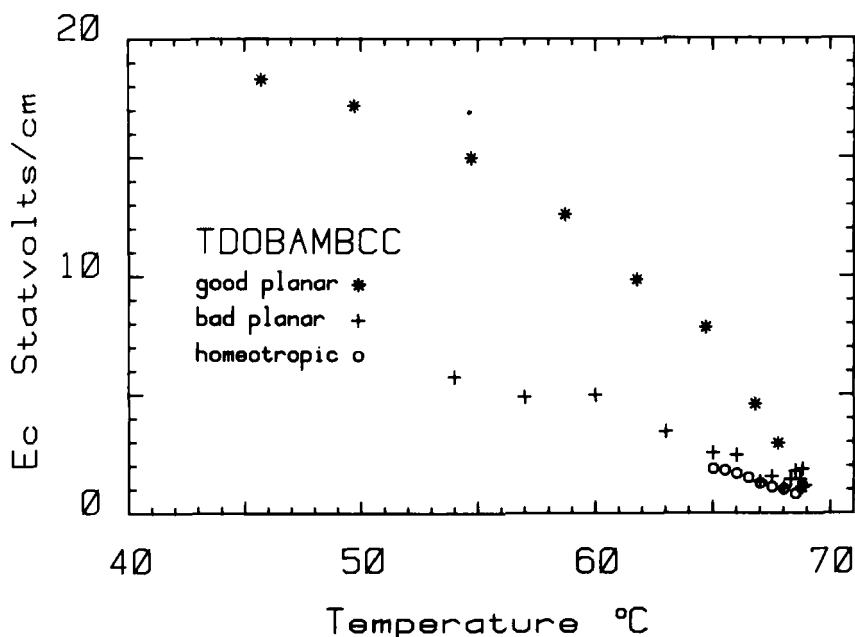


FIGURE 27 Unwinding critical DC field versus temperature for TDOBAMBCC in various geometries.

for this discrepancy, which may be due to a particularly large uncontrolled screening effect.

On Figure 28 we have plotted the critical field data for HOBACPC versus temperature in planar geometry. The values are an order of magnitude lower than those previously obtained for DOBAMBC, DOBAMBCC and TDOBAMBCC in the same geometry. This must be related to the fact that in this compound the chlorine group which carries the big electric dipole is directly fixed on the asymmetric carbon. The internal molecular rotations cannot decrease the spontaneous polarization, which depends only on the angular order parameter of the chiral carbon.

On Figure 29 is plotted for the OOBAMBMC the value of the critical field at two given temperatures versus the electric field frequency. At low frequency the critical RMS value of the AC field compares with the previous DC measurement of E_c . The figure shows a divergence of E_c around 400 hertz. This frequency could be the relaxation frequency¹⁴ of the molecules on the cone of angle θ . At higher frequency, the field does not vary with the frequency. We may think that, in that range of frequency, the molecules can not follow the field and so the unwinding may be only due to the induced polarization.

We can estimate the critical field E_c associated with the dielectric anisotropy (ϵ_a) coupling. We use the formula from Ref. 13: $E_c = (\pi^2/Z) (4\pi K_o/\epsilon_a)$. We

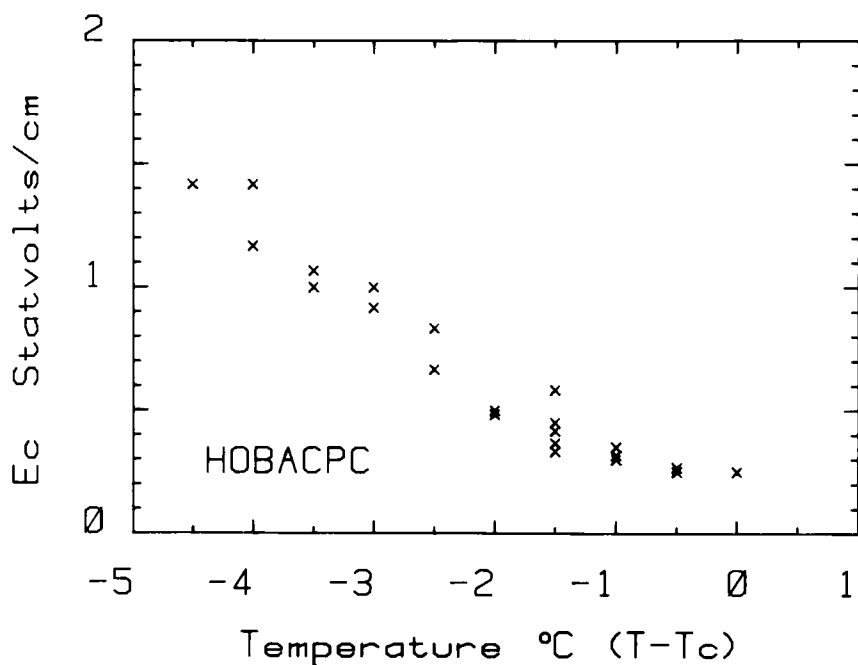


FIGURE 28 Unwinding critical DC field versus reduced temperature for HOBACPC in homeotropic geometry.

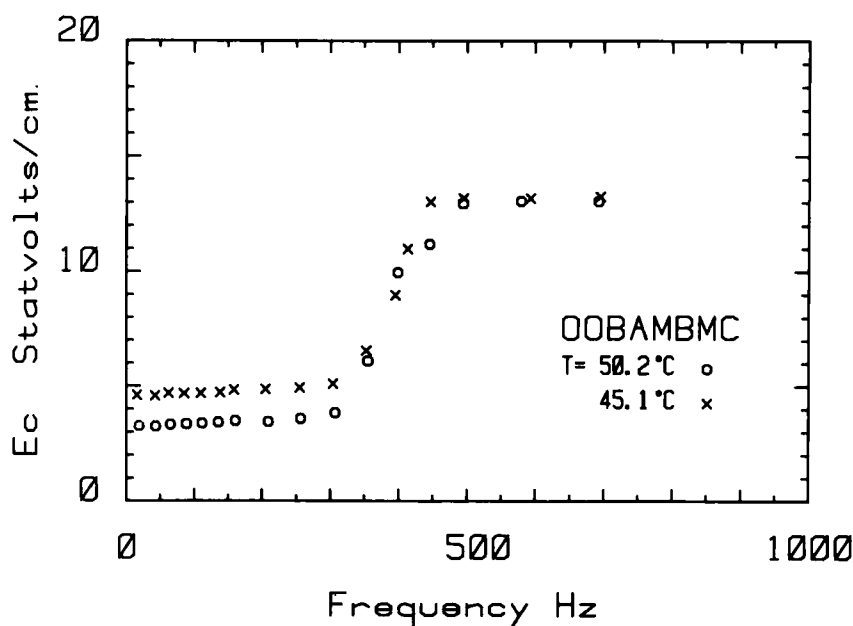


FIGURE 29 Unwinding critical AC field versus frequency for OOBAMBMC at two different temperatures.

estimate $\epsilon_a = \epsilon_{\parallel} - \epsilon_{\perp} \approx 2.4$ by analogy with DOBAMBC¹⁵ which is chemically and dielectrically comparable. Assuming $K_o \sim 5 \cdot 10^{-7}$ and $Z = 7 \mu\text{m}$ results in $E_c \sim 20$ esu, comparable to the observed value $E_c = 13$ esu.

Calculation of the spontaneous polarization

Using the value of E_c plotted on Figure 25, the obtained values of θ and Z and the dielectric anisotropy given in Ref. 15 we have calculated for various temperatures the value of $P_a K_o = (\pi^4/4) (\theta/E_c Z^2)$ (the apparent polarization coefficient P_a over K_o the elastic constant coefficient) to compare with the simple prediction previously described, and $P_i = |\epsilon_a| E_c / 4\pi\theta$ (the anisotropic part of the induced polarization), to check an eventual effect of the anisotropy of the dielectric constant. The results obtained are plotted in Figure 30, which represents the variation of P_a/K_o versus P_i , for a range of temperature of 25°C for DOBAMBC and TDOBAMBCC and only 5°C for DOBAMBCC. We observe that P_a/K_o is almost constant in such a large range of temperature. This is a good verification of the simple theoretical model: the unwinding is due to the permanent polarization. Trying to go farther and to fit these data on the law predicted in Ref. 13 is more speculative because of the small range in P_i . Within our experimental accuracy, we cannot ascertain that the small slope of P_o compared to P_i is significantly different from zero. Up to now, we have no evidence of any contribution to E_c of the dielectric anisotropy. Note that all these measurements were made in DC. The coupling of the electric field with the anisotropy of the dielectric constant is certainly an important mechanism at higher frequency, as previously shown. From now on we neglect the dielectric coupling.

To calculate P_o , we must estimate K_o . We take the value $K_o = 5 \cdot 10^{-7}$ cgs typical for nematic materials. The obtained values of P_o are shown on Table IV in esu units. To compare the permanent polarization with the dipolar moment of the molecule, P_o by molecule is also indicated on this table, using 1.2×10^{21} as the number of molecules per cm^3 .

For the four compounds without a strong dipole on the asymmetric carbon, the estimated values of P_o from homeotropic and planar geometries are very comparable, of the order of 10^{-3} Debye/rad/molecule. As previously, discussed, we must discard the erratic smallest value $0.6 \cdot 10^{-3}$ from one sample of TDOBAMBCC. For HOBACPC the estimated P_o is an order of magnitude larger.

This increase compares well with the direct measurements of P_o for the same compounds in Ref. 16, where the ratio of P_o for HOBACPC and TDOBAMBCC is about 5. The order of magnitude of P_o in DOBAMBC also deduced from direct measurement techniques¹⁷⁻²⁰ compares well with the absolute values of Ref. 16. Apart from the first experiment by Meyer,² there are no other published data of the helix unwinding critical field, close to zero frequency, so that we cannot make any serious comparison. To explain why our present esti-

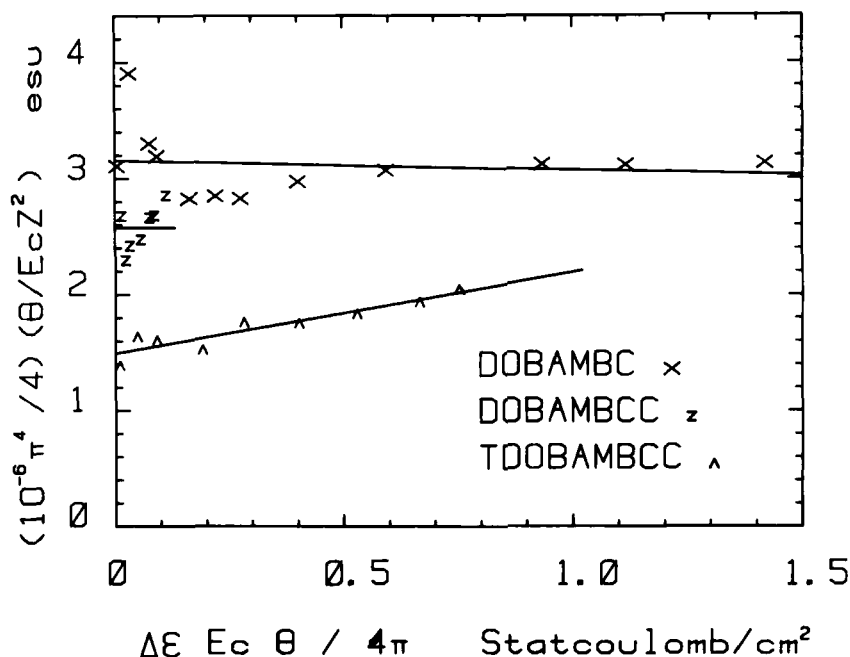


FIGURE 30 Apparent reduced spontaneous polarization versus the critical field induced polarization per unit tilt angle.

TABLE IV

P_o in Debye by radian is obtained by taking $K_o = 5 \cdot 10^{-7}$ cgs (a typical nematic elastic constant) and the number of molecules by cm^3 as $1.2 \cdot 10^{21}$

Compound	Measurement method	P_o/K_o esu	P_o Debye/Rad
DOBAMBC	Planar orientation	$3 \cdot 10^6$	$1.3 \cdot 10^{-3}$
	Homeotropic orientation	$2.9 \cdot 10^6$	$1.2 \cdot 10^{-3}$
DOBAMBCC	Planar orientation	$2.4 \cdot 10^6$	$1.0 \cdot 10^{-3}$
OOBAMBMC	Planar orientation	$3.4 \cdot 10^6$	$1.4 \cdot 10^{-3}$
TDOBAMBCC	Planar orientation		
	Well oriented sample	$1.4 \cdot 10^6$	$0.6 \cdot 10^{-3}$
	Badly oriented sample	$4.3 \cdot 10^6$	$1.8 \cdot 10^{-3}$
	Homeotropic orientation	$4.7 \cdot 10^6$	$1.9 \cdot 10^{-3}$
HOBACPC	Homeotropic orientation	$31 \cdot 10^6$	$13 \cdot 10^{-3}$

mates of P_o range one order of magnitude lower than the one obtained from the direct P_o measurement technique, we could first incriminate our choice of the twist constant K_o . We do not believe however that a choice of a larger value than the one chosen ($K_o = 5 \cdot 10^{-7}$ cgs) could be physical. We tend to think that there could be a systematic effect in our experiments which would increase the unwinding field. For instance, there could be a screening effect from free ions which could lower the apparent electric field seen by the dipoles in the bulk of the sample. An increase in the electric field frequency could be useful to check this point. The trouble is that up to now, we do not know of any model to describe the helix unwinding in AC electric field.

CONCLUSION

In this work, we have made a systematic study of some geometrical and electrical properties of chiral smectic C* compounds from the same chemical family.

The tilt angle of the molecules in the layers has been measured by three methods: one in the helical structure by an X-ray technique, the two others in the texture unwound by an electric field. Within the experimental accuracy, the tilt angle is the same in the helical as in the unwound textures. The differences in the molecular formulae of the studied compound family do not result in significant changes in the tilt angle. The tilt depends on the departure from the transition temperature according to a power law $(T_c - T)^\beta$ with $\beta \sim 0.35$. The accuracy on β is not very good, because of a T_c shift due to sample deterioration. However we can discard the mean field value $\beta = 0.5$. This non classical value of β is confirmed by a recent work of the Russian group.²¹

The helical texture pitch shows a general decrease with decreasing temperature. It follows an hyperbolic law versus the square of the tilt angle. The parameters of the hyperbolas are different for the different compounds. Nevertheless, the limit values at low temperature are between two and four microns for all studied compounds except one. That one, which has a symmetric chemical formula (PACMB), shows a pitch divergence four degrees below the transition temperature with a change of the helix sense of rotation.

The electrical field necessary to unwind the helix has been measured. It increases with decreasing temperature and is of the order of ten statvolts by cm, ten degrees below the transition temperature. A simple model of the unwinding allows us to connect that field with the permanent polarization, the dielectric anisotropy, a twist elastic constant, the tilt angle of the molecules and the pitch of the helical structure. Using this model, the permanent polarization has been estimated for the different compounds. The obtained values indicate that a polar group of some Debye substituted on the central part of the molecule results in a permanent polarization by molecule of 10^{-3} and on the chiral

part of 10^{-2} Debye/rad. We think that this result demonstrates the influence of intramolecular rotations, superimposed to intermolecular rotations, on the polar order parameter of chiral smectic C* liquid crystals. There remains an unexplained discrepancy of one order of magnitude between our estimates of the spontaneous polarization and the direct measurements of the literature. Further experiments are obviously necessary, but our values of critical field, which are reproducible, remain useful for people interested in electric field applications.

Acknowledgments

We thank Dr. Liebert and P. Keller for the supply of good quality samples and help in the optical tilt measurements.

References

1. P. G. de Gennes, *The Physics of Liquid Crystals*, (Clarendon Press, Oxford), (1974).
2. R. B. Meyer, L. Liebert, L. Strzelecki and P. Keller, *J. de Phys. Lett.*, **36**, 69 (1975).
3. P. Keller, L. Liebert and L. Strzelecki, *J. de Phys. Coll.*, **37**, C3-27 (1976). P. Keller, Thèse de 3ème Cycle, Université Paris-Sud, (1977).
4. G. Durand and Ph. Martinot-Lagarde, *Ferroelectrics*, **24**, 89 (1980).
5. J. Doucet, A. M. Levelut and M. Lambert, *Mol. Cryst. Liq. Cryst.*, **24**, 317 (1974).
6. R. Bartolino, G. Durand and J. Doucet, *Ann. de Phys.*, **V3**, 257 (1978).
7. S. Ma, *Modern theory of critical phenomena* (Benjamin, Reading, Mass., 1976). G. Toulouse and P. Pfeuty, "Introduction to the renormalization group and to critical phenomena" (Wiley, New York, 1977).
8. Draper and Smith, *Applied Regression Analysis*, (Wiley and Sons, New York, 1966).
9. B. I. Ostrovskii, A. Z. Rabinovich, A. S. Sonin, B. A. Strukov and N. I. Chernova, *JETP Lett.*, **25**, 70 (1977).
10. Y. Galerne, *J. de Phys.*, **39**, 1311 (1978).
11. Ph. Martinot-Lagarde, *J. de Phys. Colloq.*, **37**, C3-129 (1976).
12. W. Urbach, M. Boix and E. Guyon, *Appl. Phys. Lett.*, **25**, 479 (1974).
13. Ph. Martinot-Lagarde, Proceeding of the Eighth International Liquid Crystal Conference, Kyoto, July 1980. (To be published in *Mol. Cryst. Liq. Cryst.*)
14. Ph. Martinot-Lagarde and G. Durand, *J. de Physique*, Feb. 1981 (to be published).
15. D. S. Parmar and Ph. Martinot-Lagarde, *Ann. Phys.*, **V3**, 275 (1978).
16. L. Petit, P. Pieranski and E. Guyon, *C.R.A.S.*, Paris, **284**, 535 (1977).
17. Ph. Martinot-Lagarde, *J. de Physique Lett.*, **38**, L-17 (1977).
18. B. I. Ostrovskii, A. Z. Rabinovich, A. S. Sonin and B. A. Strukov, *JETP*, **47**, 912 (1978).
19. J. Hoffman, W. Kuczynski and J. Malecki, *Mol. Cryst. Liq. Cryst.*, **44**, 287 (1978).
20. K. Yoshino, T. Uemoto and Y. Inuishi, *Jap. J. Applied Phys.*, **16**, 571 (1977).
21. B. J. Ostrowsky, A. Z. Rabonivich, A. S. Sonin, E. L. Sorkin, B. A. Strukov and S. A. Tabaskin, *Ferroelectrics*, **24**, 309 (1980).